

Marquette University

e-Publications@Marquette

---

Master's Theses (2009 -)

Dissertations, Theses, and Professional  
Projects

---

## Profile Synthesis of Prismatic-Prismatic Variable Joints for Use In Reconfigurable Mechanisms

Ryan Daniel Callahan  
*Marquette University*

Follow this and additional works at: [https://epublications.marquette.edu/theses\\_open](https://epublications.marquette.edu/theses_open)



Part of the [Engineering Commons](#)

---

### Recommended Citation

Callahan, Ryan Daniel, "Profile Synthesis of Prismatic-Prismatic Variable Joints for Use In Reconfigurable Mechanisms" (2019). *Master's Theses (2009 -)*. 622.  
[https://epublications.marquette.edu/theses\\_open/622](https://epublications.marquette.edu/theses_open/622)

PROFILE SYNTHESIS OF PRISMATIC-PRISMATIC VARIABLE JOINTS FOR  
USE IN RECONFIGURABLE MECHANISMS

by

Ryan D. Callahan, B.S.

A Thesis Submitted to the Faculty of the  
Graduate School, Marquette University,  
in Partial Fulfillment of the Requirements for  
the Degree of Master of Science

Milwaukee, Wisconsin

May 2019

## **ABSTRACT**

### **PROFILE SYNTHESIS OF PRISMATIC-PRISMATIC VARIABLE JOINTS FOR USE IN RECONFIGURABLE MECHANISMS**

Ryan D. Callahan, B.S.

Marquette University, 2019

Reconfigurable mechanisms provide increased flexibility in machine design and can be used in a variety of applications. Variable joints in reconfigurable mechanisms allow for machine designs that better optimize space and resources. This thesis uses a configuration space analysis to determine the motion profiles of Prismatic-Prismatic higher variable joints. Prismatic-Prismatic variable joints have never been analyzed or synthesized. In addition, no variable joints of any type have been considered with two-dimensional contact points. Variable joints enable the creation of Type II Mechanisms with Variable Topology, mechanisms whose topology changes due to changes in joint geometry. The goal of this synthesis is to synthesize Prismatic-Prismatic variable joints with one and two-dimensional contacts, outline their designs, and determine the design restrictions for each variation.

## ACKNOWLEDGMENTS

Ryan D. Callahan, B.S.

This degree was only made possible due to the help and support of many people.

Dr. Philip Voglewede, for giving me incredible guidance through this process with constant enthusiasm. He has driven me to grow as a student and an engineer.

Kristina, for her love and encouragement. Continuously supporting me and motivating me throughout this process.

Family and friends, for supporting my education and stirring my curiosity throughout my life.

## TABLE OF CONTENTS

<b>ACKNOWLEDGMENTS</b> . . . . .	<b>i</b>
<b>LIST OF TABLES</b> . . . . .	<b>vi</b>
<b>LIST OF FIGURES</b> . . . . .	<b>vii</b>
<b>CHAPTER 1 Introduction</b> . . . . .	<b>1</b>
1.1 Motivation . . . . .	1
1.2 Thesis Overview . . . . .	4
<b>CHAPTER 2 Literature Review</b> . . . . .	<b>6</b>
2.1 Classical Joint Design and Classification . . . . .	7
2.2 Joint Classification . . . . .	8
2.2.1 Lower Pairs . . . . .	8
2.2.2 Higher Pairs . . . . .	8
2.2.3 Prismatic Higher Pair Classification . . . . .	9
2.3 Classification of Reconfigurable Mechanisms . . . . .	11
2.4 Mechanism Analysis . . . . .	13
2.4.1 Classical Mechanism Analysis . . . . .	13
2.4.2 Reconfigurable Mechanism Analysis . . . . .	14
2.5 Variable Joint Synthesis and Implementation . . . . .	15

2.5.1	Variable Joint Synthesis . . . . .	15
2.5.2	Mechanism Synthesis . . . . .	16
2.6	Configuration Space Analysis . . . . .	17
2.7	Summary . . . . .	18
<b>CHAPTER 3 Methodology . . . . .</b>		<b>20</b>
3.1	Background . . . . .	20
3.2	Numerical Approach . . . . .	22
3.3	Geometric Approach . . . . .	25
3.4	Summary . . . . .	28
<b>CHAPTER 4 Verification of the Synthesis of Prismatic Higher Pairs</b>		<b>31</b>
4.1	General Assumptions . . . . .	31
4.2	Configuration Space Analysis of $P_1$ Joint . . . . .	33
4.3	Configuration Space Analysis of $P_2$ Joint . . . . .	34
4.4	Summary . . . . .	36
<b>CHAPTER 5 Prismatic-Prismatic Joint Synthesis With Point Con-</b>		<b>38</b>
<b>tacts . . . . .</b>		<b>38</b>
5.1	Desired Motion Path . . . . .	38
5.2	Valid and Invalid Prismatic-Prismatic Variable Joint Types . . . . .	40
5.2.1	$P_1P_1$ Variable Joints . . . . .	42
5.2.2	$P_1P_2$ and $P_2P_1$ Variable Joints . . . . .	48

5.2.3	$P_2P_2$ Variable Joints . . . . .	51
5.3	Summary . . . . .	52
<b>CHAPTER 6 Prismatic-Prismatic Joint Synthesis With Circular Con-</b>		
<b>tacts . . . . .</b>		<b>55</b>
6.1	Preliminaries . . . . .	55
6.2	Valid and Invalid Prismatic-Prismatic Variable Joint Types . . . . .	56
6.2.1	$P_1P_1$ Variable Joints . . . . .	56
6.2.2	$P_1P_2$ and $P_2P_1$ Variable Joints . . . . .	59
6.2.3	$P_2P_2$ Variable Joints . . . . .	60
6.3	Numerical Analysis of Prismatic-Prismatic Variable Joints . . . . .	60
6.3.1	$P_1P_1$ Variable Joints . . . . .	61
6.3.2	$P_1P_2$ Variable Joints . . . . .	63
6.3.3	$P_2P_2$ Variable Joints . . . . .	63
6.4	Comparison of Prismatic-Prismatic Variable Joints . . . . .	67
6.5	Summary . . . . .	69
<b>CHAPTER 7 Potential of a Revolute-Prismatic-Prismatic Variable</b>		
<b>Joint . . . . .</b>		<b>70</b>
7.1	$R_nP_1P_1$ Joints . . . . .	70
7.2	$R_nP_1P_2$ Joints . . . . .	71
7.3	$R_nP_2P_2$ Joints . . . . .	71
7.4	Summary . . . . .	73

<b>CHAPTER 8 Summary and Future Work</b> . . . . .	<b>75</b>
8.1 Contributions . . . . .	75
8.2 Future Work . . . . .	76
<b>APPENDIX A Matlab Code</b> . . . . .	<b>79</b>
A.1 Geometric Analysis of Higher Pairs and Variable Joints . . . . .	79
A.2 Configuration Space Analysis of $P_2P_2$ With 2-D Contacts . . . . .	81
<b>References</b> . . . . .	<b>85</b>



## LIST OF TABLES

5.1	Summary of analysis of various Prismatic-Prismatic variable joints with point contacts . . . . .	41
5.2	Coordinates of point contacts for moving link of a $P_1P_1$ variable joint . .	46
5.3	Coordinates of point contacts for moving link of a $P_1P_2$ variable joint . .	51
5.4	Coordinates of point contacts for moving link of a $P_2P_2$ variable joint . .	52
5.5	Summary of analysis of various Prismatic-Prismatic variable joints with point contacts . . . . .	54
6.1	Summary of analysis of various Prismatic-Prismatic variable joints with circular contacts . . . . .	57

## LIST OF FIGURES

2.1	Diagram of $P_1$ higher pair . . . . .	11
2.2	Diagram of $P_2$ higher pair . . . . .	11
3.1	Example of how a configuration space analysis works, showing the locations of valid configurations . . . . .	21
3.2	A series of valid configuration points with the inner object at $0^\circ$ . . . . .	25
3.3	A series of valid configuration points with the inner object at $-10^\circ$ . . . . .	26
3.4	Flow chart of the numerical program . . . . .	27
3.5	An example $P_1$ higher pair with its corresponding configuration space boundaries; all space outside these boundaries is valid . . . . .	28
3.6	A stationary object for a $P_2P_2$ variable joint with the boundaries for a geometric configuration space analysis . . . . .	29
3.7	An example of a valid configuration in the geometric approach combined with the numerical approach . . . . .	29
3.8	An example of an invalid configuration in the geometric approach combined with the numerical approach . . . . .	30
4.1	Results of Slaboch's configuration space analysis of $P_1$ joints [2] . . . . .	32
4.2	Validation of Slaboch's configuration space analysis of $P_1$ joints . . . . .	33
4.3	Results of Slaboch's configuration space analysis of $P_2$ joints [2] . . . . .	35
4.4	Validation of Slaboch's configuration space analysis of $P_2$ joints . . . . .	36
5.1	Diagram of the motion path of a Prismatic-Prismatic variable joint . . . . .	39

5.2	Definition of the first and second pair of a Prismatic-Prismatic variable joint	42
5.3	Diagram of $P_1P_1$ first variation with point contacts and a large offset of the bottom of the stationary link . . . . .	43
5.4	Diagram of $P_1P_1$ first variation with point contacts and a smaller offset of the bottom of the stationary link . . . . .	43
5.5	Diagram of $P_1P_1$ second variation with point contacts . . . . .	45
5.6	Geometric configuration space analysis of the second portion of the second variation of a $P_1P_1$ at $-10^\circ$ (CCW) (left), $0^\circ$ (center), and $10^\circ$ (CW) (right)	45
5.7	Diagram of $P_1P_1$ third variation with point contacts shown as the moving link moves from (1) to (4) . . . . .	47
5.8	Diagram of $P_1P_2$ with point contacts . . . . .	49
5.9	Diagram of $P_1P_2$ with point contacts and no offset in the stationary link	50
5.10	Diagram of $P_2P_2$ with point contacts . . . . .	53
6.1	Diagram of $P_1P_1$ with circular contacts and no offset . . . . .	58
6.2	Diagram of $P_1P_1$ with circular contacts and an offset . . . . .	59
6.3	Sample $P_2P_2$ with point contacts . . . . .	60
6.4	Sample $P_2P_2$ with circular contacts . . . . .	60
6.5	Maximum undesired rotations of $P_1P_1$ joints with respect to changes in contact radius and translation angle . . . . .	62
6.6	Configuration space of a $P_2P_2$ in the $x$ and $\psi$ directions . . . . .	65
6.7	The maximum $\psi$ error from the desired motion path for each corresponding $x$	65
6.8	Maximum undesired rotations of a $P_2P_2$ variable joint with respect to various factors. . . . .	66

7.1	Analysis of a $P_1P_1$ variable joint with a Revolute pair . . . . .	71
7.2	Diagram showing the interference caused by a $R_nP_1P_2$ joint . . . . .	72
7.3	Diagram of a $R_nP_2P_2$ joint, showing the two contact points available for the initial prismatic motion . . . . .	73

## CHAPTER 1

### Introduction

#### 1.1 Motivation

Reconfigurable mechanisms are mechanisms that are able to change their topology. This can allow for a single mechanisms to serve multiple functions, creating a more efficient use of weight, space, and material.

Reconfigurable mechanisms can reduce the cost of machinery for a company in two ways: capital costs and operating costs. Actuators and the associated drives are often one of the most expensive initial costs of a machine or robot depending on a need for greater force, speed, acceleration, and/or accuracy. The use of reconfigurable mechanisms can reduce the number of actuators depending on the needed motion paths. If the actuator being eliminated would have needed to be moved itself, it can also reduce the force needed from that actuator, further reducing the cost. Not only are actuators one of the more expensive parts when purchasing a machine initially, they directly lead to the majority of the machine's operating costs in the form of electricity. For large manufacturing machinery running 24 hours per day, these costs can add up to significant sums.

Every additional actuator leads to an increase of complexity which also adds costs. Reducing the complexity of machinery reduces machine downtime. This downtime leads to lost productivity, especially for machines expected to run constantly. From a physical layout, designing the machinery around actuators can become complex depending on the kinematic arrangement of the machine, especially if the actuator needs to be attached to a moving axis itself. From a programming perspective, the complexity for each additional axis is magnified. This complexity directly leads to an increase in the difficulty to service the machine. Physical damage to an actuator can often be difficult to diagnose and many times can be mistaken for an issue in the programming. Each actuator also has a drive, which in themselves are complex components, further adding failure points for the machine.

Reconfigurable mechanisms can create more flexible machinery, providing industry with more robust tools that are more adaptable to changes. More robust machinery also allows the machinery to adapt to various product lines and different needs over time, making them more capable over the long term. Problems with physical joints are easier to diagnose and repair, especially for millwrights trained in repairing traditional mechanical machine components. These reasons combined with the lower capital and operating costs made possible by reconfigurable mechanisms allows for companies to expand their use of automation. Automation allows companies to reduce costs, allowing for increased profit margins.

Automation is increasingly becoming more and more a part of life, especially in manufacturing. The ever-growing need for automation has led to a need for more robots capable of performing complex motion. For robots to do more tasks, robot manufacturers typically add more degrees of freedom and, in turn, more actuators. Reconfigurable robots and mechanisms can simplify machines by allowing for fewer actuators to create complex motion paths which typically require the use of larger degree of freedom machines.

Reconfigurable mechanisms have the capability to revolutionize robotics and machinery; however, the field remains immature with significant opportunities for advancement to achieve its potential. A major part of this gap is in the synthesis of variable joints. Type II Mechanisms with Variable Topology are reconfigurable mechanisms whose geometry allows for a change in topology, which requires a variable joint. Prismatic-Prismatic variable joints are a type of variable joint that have yet to be systematically synthesized, a vital first step before its implementation and application. A thorough synthesis of Prismatic-Prismatic variable joints requires defining the desired motion path and outlining the design constraints and restrictions to achieve that desired motion path. The effects of non-ideal joint geometry and physical implementation need to be analyzed further to provide design constraints. Understanding the design constraints of these variable joints is crucial to being able to design them and implement them into

reconfigurable mechanisms. This work advances the design of variable joints as well as reconfigurable mechanisms as a whole, a rapidly expanding field.

This thesis will contribute a complete analysis of Prismatic-Prismatic variable joints. This thesis will analyze Prismatic-Prismatic variable joints consisting of higher pairs with both one-dimensional and two-dimensional circular contact points. This analysis will result in a synthesis of Prismatic-Prismatic variable joints. Prismatic-Prismatic variable joints will also be analyzed in conjunction with Revolute-Prismatic variable joints to determine their feasibility.

## **1.2 Thesis Overview**

Chapter 2 overviews the pertinent previous work relevant to this thesis. This previous work includes the foundation of mechanical joints, mechanisms, and how they are synthesized. Previous work on reconfigurable mechanisms are also outlined along with how this work relates to the work of this thesis. Works on configuration space analysis are presented as these provide a tool for the synthesis performed in this thesis.

In Chapter 3, the configuration space method used for the synthesis throughout the thesis is outlined. Explaining the methodology used helps illustrate



how the synthesis of variable joints is done, as well as illuminating why the configuration space method was used.

In Chapter 4, the methodology outlined in Chapter 3 is used to validate prior research of valid prismatic higher pair configurations. These configurations are the basis of this research; validating these configurations allows for the synthesis of Prismatic-Prismatic variable joints performed in this thesis.

In Chapter 5, a configuration space method is used to investigate Prismatic-Prismatic variable joints while using ideal one-dimensional contact points. This analysis produces the design constraints of these joints.

In Chapter 6, the configuration space method is repeated for Prismatic-Prismatic variable joints while using circular contacts. The effect of circular contacts and the undesirable motions they can cause will be quantified to determine whether or not the variable joint has the potential to jam.

In Chapter 7, the Prismatic-Prismatic variable joints will be combined with the constraints of Revolute-Prismatic variable joints. Chapter 7 will determine the feasibility of these joints.

In Chapter 8, the contributions to the field of this thesis will be reviewed and outlined.

## CHAPTER 2

### Literature Review

The goal of this thesis is to synthesize Prismatic-Prismatic variable joints for their design and implementation into reconfigurable mechanisms. Before synthesizing variable joints, it is important to identify the need for the synthesis. A proper literature review not only identifies holes in the current state of the art but shows possible research avenues for the work. In addition to identifying need, it is vital to establish the foundation methodologies that can be used to perform the synthesis.

A proper understanding of classical joint design is the foundation of variable joint design and many of the same principles are applicable in this thesis. It is also important to paint a picture of what reconfigurable mechanisms are, how they are analyzed, and how variable joints allow for reconfigurable mechanisms to be created. Previous works, specifically with regards to variable joints and mechanisms that use them, are necessary as they are the most closely related precursors to this research and have many parallels between their synthesis. Finally, the work outlining the methodology for configuration space analyses, the primary tool used for the synthesis of Prismatic-Prismatic variable joints, is presented.

## 2.1 Classical Joint Design and Classification

Reuleaux [9] created the foundation to modern kinematics. With respect to this research, the most important aspects of his work were the creation of the notion of kinematic pairs, i.e., two individual machine elements that interact with each other. A machine element in this context is a broad term for the elementary components of a machine, like joints, bearings, gears, etc. These pairs are then further classified by Reuleaux into lower pairs and higher pairs. For a pair of elements to be considered a lower pair, they must have surface to surface contact between them as opposed to a point contact; the second element must be carried upon by or enveloped by the other. These works on classical joint design and classification are the foundation of this thesis.

This designation of lower pairs has served as the paradigm for the design of robots for numerous years. The 6 lower pairs (revolute, prismatic, cylindrical, helical, spherical, and planar) are fundamental to modern mechanics and are used consistently in classical mechanism analysis and synthesis. The preliminary analysis was done by Reuleaux [9] and Kennedy [1] in the 19th century and continues to be used in modern analysis of reconfigurable mechanisms by people like Tsai [14].

Higher pairs do not require the surface contact that lower pairs need; they merely require point contacts. Higher pairs are extremely important as they open

new design paradigms of reconfigurable mechanisms, especially with regards to reconfigurable mechanisms with variable joints.

## **2.2 Joint Classification**

### **2.2.1 Lower Pairs**

According to Reuleaux [9], closed pairs must follow three rules:

1. The two elements must have surface to surface contact.
2. The two elements must be geometrically identical.
3. One element restricts the motion of the other link to the required motion.

Reuleaux used this definition to outline the six possible types of lower pair joints: revolute, prismatic, helical, spherical, planar, cylindrical. These are denoted by  $R$ ,  $P$ ,  $H$ ,  $S$ ,  $E$ , and  $C$ , respectively.

### **2.2.2 Higher Pairs**

Reuleaux also defined higher pair joints. For joints to be higher pairs, they must follow two rules:

1. The two elements must have a point or line contact.

2. The two elements must restrict relative sliding.

In this thesis, only higher pair joints will be analyzed due to the flexibility they have in design of variable joints; flexibility that is particularly advantageous to variable joints. A lower pair's requirement for surface contact limits the ability to design complex variable joints.

### 2.2.3 Prismatic Higher Pair Classification

Slaboch [2] created a notation for the types of higher pair prismatic and revolute joints that are possible without redundancies, configurations with no unnecessary contacts. A higher pair can be classified by a notation of the format  $X_u$ .  $X$  denotes the type of joint it is (e.g.,  $R$  for revolute,  $P$  for prismatic, etc). The  $u$  subscript indicates what version of the joint it is, as defined by Slaboch [2]. For a subscript of 1, the contacts are external. For a subscript of 2, the contacts are internal. For a subscript of 3, the contacts are a combination of external and internal. A type 3 joint is valid for a revolute higher pair but is redundant for a prismatic higher pair. Slaboch [2] outlined the versions of revolute and prismatic higher pairs. For prismatic higher pairs, there are two versions,  $P_1$  and  $P_2$ . These two versions restrict a translating link to translational motion without any redundant contacts.

A  $P_1$  type joint is shown in Figure 2.1. A  $P_1$  higher pair requires only two

contact bodies to maintain translational motion, denoted in Figure 2.1 as  $c_1$  and  $c_2$ . These contacts are placed on the outside of a stationary link consisting of two horizontal lines. In the Figure 2.1, the stationary link is represented by blue lines. The two circles are the “point contacts” that are connected via the dotted line and translate horizontally. Whether the point contacts are considered stationary or the horizontal lines are is arbitrary as motion is relative.

A  $P_2$  type joint can be seen in Figure 2.2. A  $P_2$  higher pair requires three contacts to maintain translational motion. These point contacts are placed internal to the stationary link. These constraint bodies must be arranged such that the point isolated on one side ( $c_3$  in this case) is attached between the two on the opposite side ( $c_1$  and  $c_2$  in this case). As with a  $P_1$  type joint, whether the circular contacts or lines are stationary is arbitrary.

The notation used to designate variable joints were defined by Slaboch [2]. For variable joints, they are denoted as  $X_u Y_v$ , combining the notation of higher pairs.  $X$  and  $Y$  denote the type of higher pair while the  $u$  and  $v$  denote the version of the higher pair.

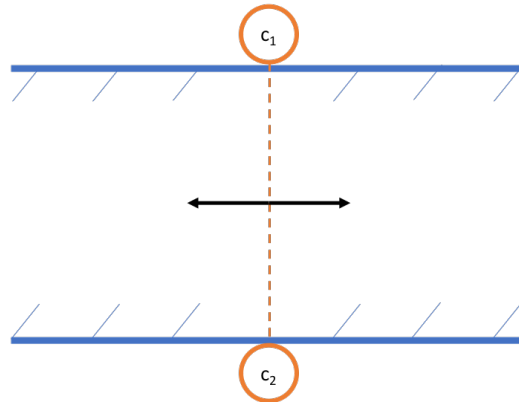


Figure 2.1: Diagram of  $P_1$  higher pair, the dashed line designates that the contacts are fixed relative to each other.

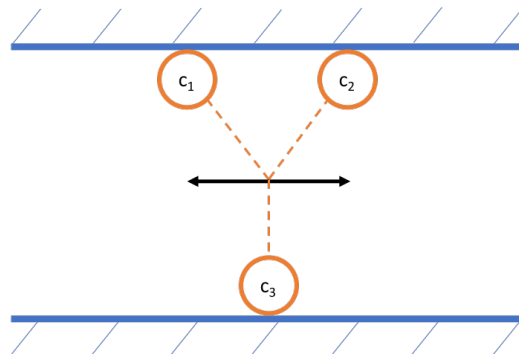


Figure 2.2: Diagram of  $P_2$  higher pair, the dashed line designates that the contacts are fixed relative to each other.

### 2.3 Classification of Reconfigurable Mechanisms

Reconfigurable mechanisms can be categorized into three categories: Metamorphic mechanisms as defined by Dai and Jones [4], Kinematotropic mechanisms as defined

by Wohlhart [18], and Mechanisms with Variable topology as defined by Kuo [5].

These are further explained below.

- **Metamorphic Mechanism:** A mechanism whose the total number of effective links changes as the mechanism moves from one configuration to another or a singular condition makes it behave differently [4]. As the mechanism moves through its motion path, some of the links disengage from the moving link allowing for a differing motion path.
- **Kinematotropic Mechanisms:** Mechanisms that, in passing a singular position in which a certain transitory infinitesimal mobility is attained, permanently change their global mobilities. A Kinematotropic Mechanism intrinsically has a singularity designed into it, and can pass through that singularity, creating a different motion profile.
- **Mechanism with Variable Topology (MVT):** A mechanisms with variable topology is a mechanism whose topology changes during operation. MVTs can be classified into three main types according to Shieh, Sun, and Chen [15] :
  1. MVTs that change topology due to an intrinsic constraint (Kinematotropic or Metamorphic).
  2. MVTs that change topology due to joint geometry.



3. MVTs that change topology due to an external constraint  
(Metamorphic).

Type II MVTs are the most important to this research as they require a variable joint to be made possible. A variable joint is a combination of two higher pair joints. Synthesizing more types of variable joints allows for more Type II MVTs to be designed.

## **2.4 Mechanism Analysis**

Most analyses of reconfigurable mechanisms is based on methods of analysis of classical mechanisms. Classical mechanisms have been rigorously analyzed since the 19th century and the analysis of these mechanisms has continued since. With the advent of reconfigurable mechanisms, the application of the same tools developed for classical mechanisms has been adapted and applied to reconfigurable mechanisms.

### **2.4.1 Classical Mechanism Analysis**

Gogu [1] (and similarly by Waldron [17][16]) looked at the different methods for analyzing mobility of classical, non-reconfigurable, mechanisms. Gogu analyzes a single system by using thirty-five different mobility calculation equations. All of these equations are somewhat derived from Gruebler's equation. This work is more

centered on the analysis of mechanisms in terms of classification and determining degrees of freedom for classical mechanisms. While Gogu's work doesn't directly apply to the work of this thesis, it does illustrate a common approach for analyzing mechanisms as a whole.

Tsai [14] used matrices to enumerate classical kinematic mechanisms, using classical lower pair (non-variable) joints. He analyzed a series of classical mechanisms by representing them with graph representations (i.e., mechanism schematics) as well as matrix representation. These mechanisms span from gear trains to automotive mechanisms to robotic mechanisms. And while this work is important, and can provide significant insight into the analysis of kinematic mechanisms, this work is not usually directly applied to the synthesis of variable joints.

#### **2.4.2 Reconfigurable Mechanism Analysis**

Dai and Jones [4] adapted Tsai's work to reconfigurable mechanisms. Their matrix analysis is similar to Tsai's but is able to specifically represent reconfigurable mechanisms, in this case, metamorphic mechanisms. While this work analyzes reconfigurable mechanisms, they only investigate metamorphic mechanisms, which do not require variable joints.

Dai and Jones' work was continued further by Yan and Kuo [19] and Lan

and Du [6], for different types of reconfigurable mechanisms, namely MVTs. Being able to enumerate MVTs demonstrates how mechanisms may need variable joints to exist. Being able to quantitatively determine a need for variable joints is important, but these works do not look at variable joints themselves, nor the synthesis of these joints.

Slaboch and Voglewede [13] showed the limitations of the analysis approaches with their development of Mechanism State Matrices, a classification tool of reconfigurable mechanisms. However, this work does not specifically look at the synthesis of variable joints.

All of the work into the analysis of reconfigurable mechanisms are important precursors to the research of this thesis as they help demonstrate the need for variable joints as well as the tools to analyze them. Reconfigurable mechanism analyses help show limitations of traditional mechanisms as well as show how reconfigurable mechanisms can be designed using variable joints.

## **2.5 Variable Joint Synthesis and Implementation**

### **2.5.1 Variable Joint Synthesis**

The majority of the work on variable joints has only recently been performed.

Slaboch [2] designed the motion profiles of prismatic and revolute higher pair joints

and outlined the different configurations for both prismatic and revolute joints. These different configurations varied the locations of the moving point contacts relative to the stationary link. These configurations have the minimum number of constraint bodies necessary to form the joint without redundancies, defining the fundamental designs for these joints. These configurations and motions paths were then applied to Revolute-Prismatic ( $R_uP_v$ ) variable joints. The combinations of the configurations of each type of joint were described along with their design constraints, an example being link interference as the joint transitioned from one type to the other. This research did not investigate prismatic-prismatic variable joints or the effects of approximating obstacles as point contacts, but did provide the fundamentals of this research and a template for how a proper synthesis of variable joints should be performed.

### 2.5.2 Mechanism Synthesis

Malak [8] synthesized a Revolute-Prismatic variable joint and implemented it into a mechanism. Malak designed and built a  $RRRR$ - $RRRP$  mechanism, or a mechanism that uses a variable joint that is  $RRRR$  in one configuration, and then a  $RRRP$  in another configuration. This mechanism made use of a Revolute-Prismatic variable joint, not a Prismatic-Prismatic variable joint.

Buchta [3] performed a survey of industries to determine a Type II MVT

that could be of practical use in industry, and designed a mechanism using a Revolute-Prismatic variable joint; this work took a similar design approach to Malak. Both Malak and Buchta focused on the design of Type II MVTs and the use of Revolute-Prismatic variable joints in these mechanisms, but not on the synthesis of variable joints, Prismatic-Prismatic variable joints specifically.

Currently, no work regarding the synthesis of Prismatic-Prismatic variable joints has been performed. This thesis analyzes and synthesizes the motion profile and geometry of prismatic-prismatic higher order variable joints for their use in reconfigurable mechanisms, specifically Type II MVTs.

## **2.6 Configuration Space Analysis**

Most of the work on synthesis of variable joints has used a configuration space analysis. A configuration space is simply a two or three-dimensional area or volume that two or more rigid body objects can exist within [12]. Generally, all objects but one are moved to provide a better understanding for the mobility of the object. If multiple objects need to move relative to each other, multiple analyses can be performed and the locations at which the configuration spaces agree are the overall valid configurations for the mechanism.

Rimon and Burdick [10] [11] provided the theoretical basis behind a

configuration space analysis, specifically with regards to creating matrices characterizing two object's surfaces and their mobility with respect to each other. This work is applicable to the synthesis of variable joints as it provides a tool for this thesis.

Sacks [12] performed similar work to Rimon and Burdick, but the work was significantly more thorough in the practical implementation of configuration space approach to classical mechanisms. He used a configuration space analysis to analyze the contact of features in various mechanisms, both planar and spatial. An analysis of how tolerances relate to the configuration space method was also performed. Although he mentions higher and lower pair joints, he does not specifically use the configuration space analysis on them, nor on variable joints. Due to the more practical methodology for configuration space analysis, Sacks provides a useful tool for the synthesis of the motion profile of a prismatic-prismatic variable joint.

## **2.7 Summary**

As illustrated through the literature review, the motion path of Prismatic-Prismatic variable joints has yet to be synthesized. Since Reuleaux outlined the basics for joint and mechanism design, a significant amount of work has been done into the analysis of classical mechanisms and reconfigurable mechanisms. Slaboch pushed the study of variable joints forward through his motion profile synthesis of

Revolute-Prismatic variable joints. Malak and Buchta took the motion profiles of Revolute-Prismatic variable joints and applied them to their synthesis of Type II MVTs. All of this work has led up to the synthesis of Prismatic-Prismatic variable joints, but none have accomplished this synthesis.

## CHAPTER 3

### Methodology

This work will build upon prior research by Slaboch [2] with the use of configuration spaces and geometry. A configuration space is a collection of locations at which two or more (planar) objects can physically exist based on rigid body mechanics, essentially meaning the two objects do not overlap or deform. These locations then illustrate the potential motion path for the free object relative to the stationary objects. In the case of a joint, the configuration spaces of all of the obstacles are combined, and the union is the locations at which the mechanism can physically exist. This chapter will outline the two methodologies used in this research to synthesize Prismatic-Prismatic variable joints.

#### 3.1 Background

The configuration space analysis of Prismatic-Prismatic variable joints is performed with two different approaches: a numerical approach and a geometric approach. In the numerical approach, an algorithm written in Matlab determines if two objects are in contact with each other. The program does this by breaking the objects into line segments and then determines if any line segments overlap. If they do, it



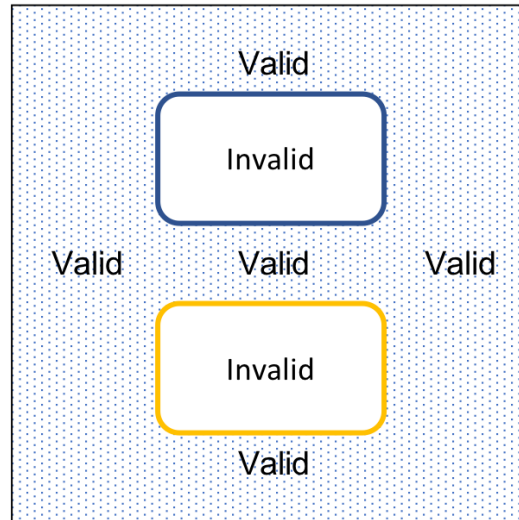


Figure 3.1: Example of how a configuration space analysis works, showing the locations of valid configurations

determines if the overlap is small enough to be able to assume surface contact. This procedure is repeated for a grid of poses to find the valid configuration space for the contact between each object. The sweep of test points is repeated for each object. The locations where the configuration spaces of each object are in union are the valid configurations as seen in Figure 3.1. The objects can then be rotated and the process repeated to get a complete picture of the valid configurations.

In the geometric approach, the geometry of the two objects is used to determine the shape of the configuration space, the locations at which one moving object can exist relative to a stationary one. The stationary object of a prismatic higher pair can be represented by a rectangle and the translating objects can be represented as circles. In configuration space, if a rectangle is interacting with a

circle of radius  $r$ , the resulting configuration space will be a rectangle with rounded corners [7]. The configuration space's height and width will be the height and width of the rectangular object plus  $2r$ , and the rounded corners of the configuration space will be of radius  $r$ . An example of this analysis will be shown later in Figure 3.5.

The two approaches for determining the configuration space of a joint can be chosen depending on the analysis. A numerical approach is better at determining the configuration space of objects with more complex geometry. It is more flexible than a geometric approach, but is more difficult to program and is an approximation (i.e., the results are not exact). If the geometries of the two objects are simple, a geometric approach is better. The geometric approach yields an exact result when looking at simpler situations, but is difficult to create 3-D volumes of configurations often caused by two-dimensional objects.

### **3.2 Numerical Approach**

A numerical approach to determine the configuration space and the resulting motion of a variable joint can be found by approximating both interacting objects as polygons. The configuration space can then be determined by finding the intersection of the polygons as they move in the plane. For the numerical approach, a Matlab program to determine if two polygons intersected was developed as there are no known built-in Matlab functions to determine when a circle contacts or

intersects a polygonal object. This program will be referred to as the Numerical Program and code for it can be found in Appendix A.

The Numerical Program determines the configuration space of various prismatic higher pairs. The program loops through a series of poses (position and orientation) to create a two or three dimensional configuration space for the joint. For this thesis, the  $x$  direction is the direction of the joint's first translation, the  $y$  direction is perpendicular to the  $x$  in the plane of the translation,  $\psi$  is the (undesired) rotations of the moving object, and  $\theta$  is the angle of translation for the second portion of the joint.

The process is summarized in the flowchart in Figure 3.4. The general program flow is as follows:

1. The two polygons representing the stationary objects and moving object are broken into line segments between each of the nodes of the polygons.
2. The polygon representing the stationary object is placed at various configurations of  $x$  and  $y$ .
3. All of the line segments of both objects are analyzed using a built in mathematical formula to determine if any two lines of the polygons representing the object intersect, and if so, where.

4. If the objects intersect, they intersect at two points. The distance between the two intersection points is determined.
  - If this distance is small based on the dimensions of the two objects and the desired accuracy, the configuration is approximated as surface contact, and the configuration is deemed to be valid.
  - If the distance is large, the polygons are said to be overlapping and the configuration is deemed invalid.
  - If the objects do not interact, it is considered valid and the stationary object is not in contact with the moving object.
5. Steps 1 through 4 are repeated for all of the bodies of the stationary object being analyzed.
6. The locations deemed valid in the configuration spaces of all of the constraints are the locations at which all constraints can coexist with the stationary link. The boundaries of the invalid space are the locations where the objects are in contact, the purpose of the analysis.
  - If the valid points of the configuration space form a contiguous line of points, the line is a motion path for the joint.
  - If there are no contiguous valid points, the joint in question is not a

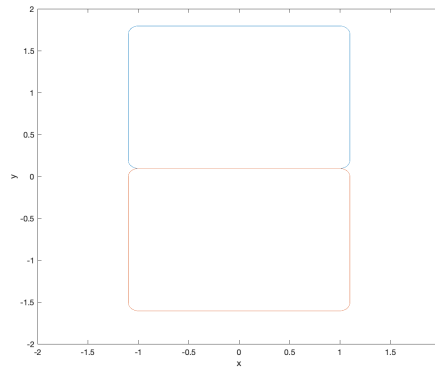


Figure 3.2: A series of valid configuration points with the inner object at  $0^\circ$

functioning variable joint for a specific  $\psi$ . (An example of this can be seen in Figures 3.2 and 3.3.)

7. Steps 1 through 6 are repeated for various rotations,  $\psi$ , of the moving object being tested, creating a three-dimensional mesh of points showing valid configurations based on the moving link's location in the  $x$ ,  $y$ , and  $\psi$ .

### 3.3 Geometric Approach

The geometric approach was implemented by using the geometry of the moving and stationary objects to determine where the configuration spaces union, showing a motion path. The approach determines the shape and dimensions of a configuration space by the dimensions and shapes of the objects that are interacting. This

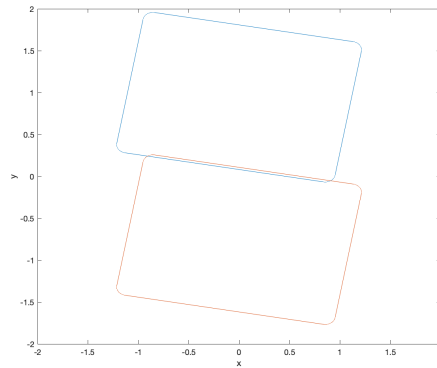


Figure 3.3: A series of valid configuration points with the inner object at  $-10^\circ$

approach is particularly useful for simple geometries, like those performed in Chapter 4. An example of this type of analysis can be seen in Figure 3.5.

The geometric approach specifically relates to analyzing prismatic-prismatic variable joints with circular objects. This approach uses the known geometry of the stationary object, and then creates boundaries the exact same distance from the stationary object as the radius of the circular objects. If the boundary has an angle greater than  $180^\circ$ , the boundary becomes rounded to the same radius as the contact points. This boundary creation can be seen in Figure 3.6.

While the geometric approach uses the geometries of the objects to determine valid configurations, it is generally combined with the numerical approach. The translating object is tested at various points, similarly to the numerical approach, and if any of the centers of the contacts of the translating

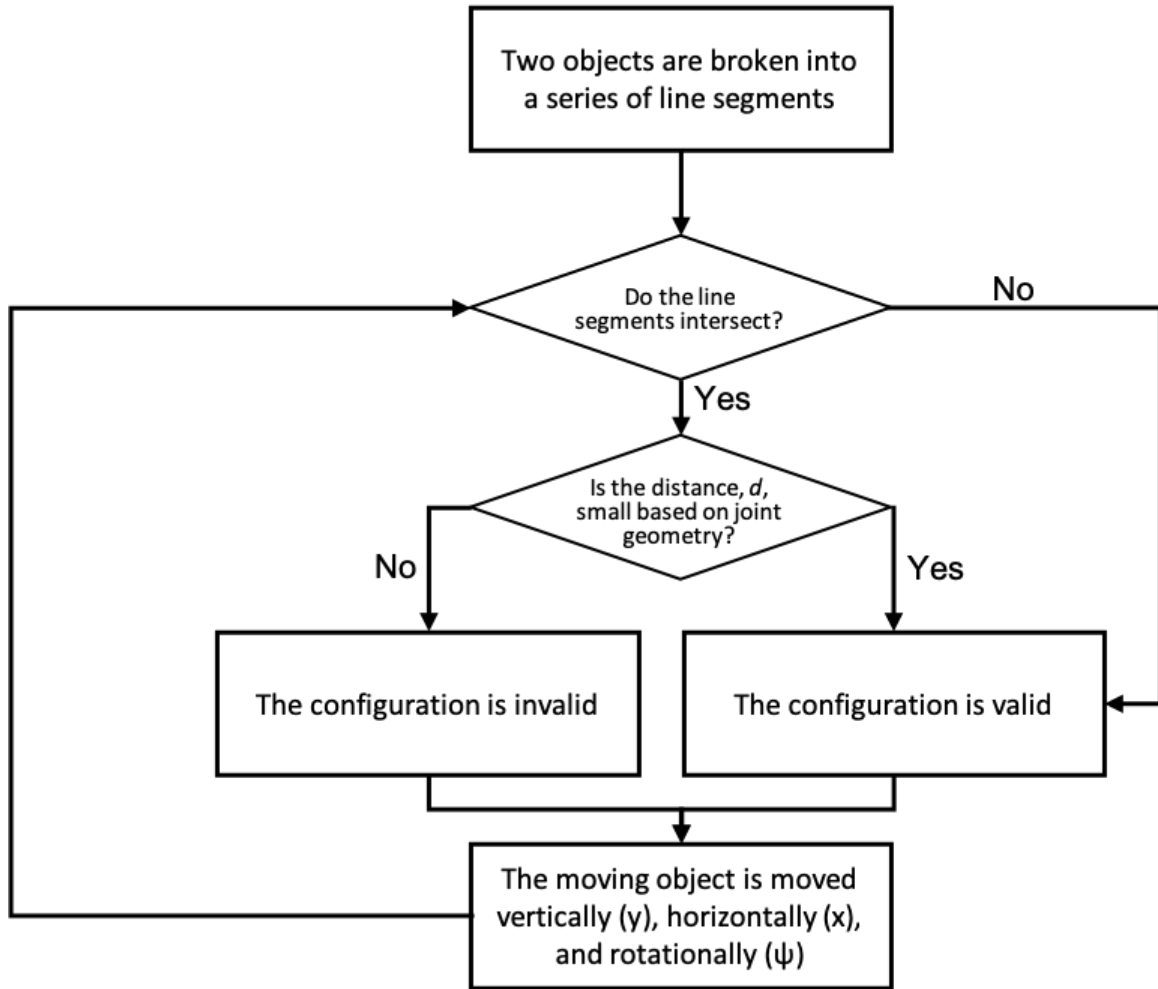


Figure 3.4: Flow chart of the numerical program

object are within the boundaries, the configuration is invalid. An example of both valid and invalid configurations is shown in Figures 3.7 and 3.8 respectively.

The geometric approach with the numerical addition is a non-exact approach similar to the numerical approach. The results are only at the poses tested. As the number of poses tested approaches infinity, the amount of error approaches zero.

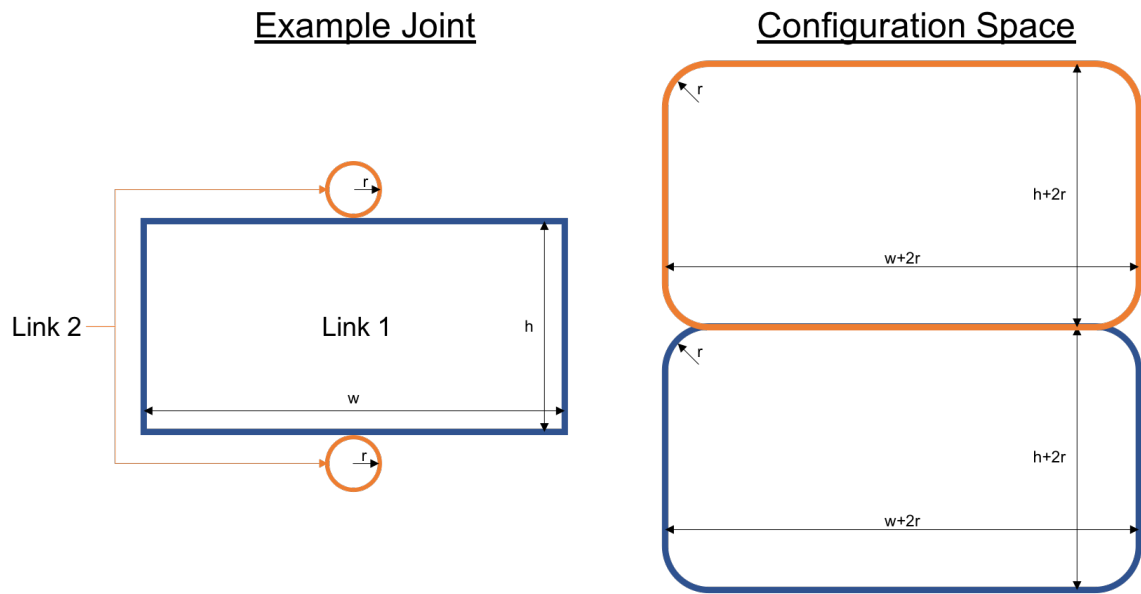


Figure 3.5: An example  $P_1$  higher pair with its corresponding configuration space boundaries; all space outside these boundaries is valid

### 3.4 Summary

This chapter overviewed the use of configuration space to analyze prismatic-prismatic variable joints in two approaches: the numerical and geometric approach. For the numerical approach, the determination of valid configurations is approximate, as the number of test points is not infinite. This approach is more exact as opposed to the numerical approach, but is less capable of extracting data and is difficult to iterate for multiple configurations like the numerical approach.

Two configuration space approaches (i.e., numerical and geometric) are combined to best analyze the motion profiles of the joints. The configuration space



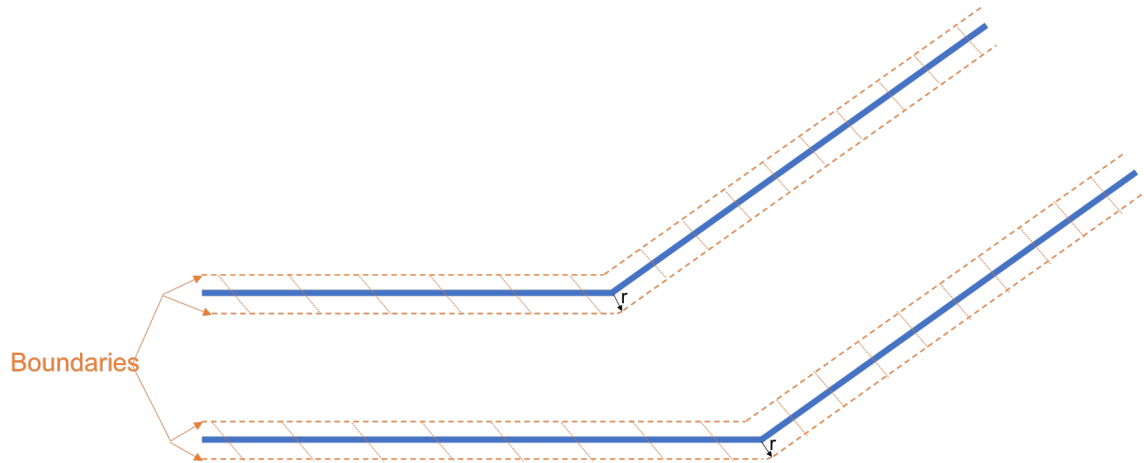


Figure 3.6: A stationary object for a  $P_2P_2$  variable joint with the boundaries for a geometric configuration space analysis

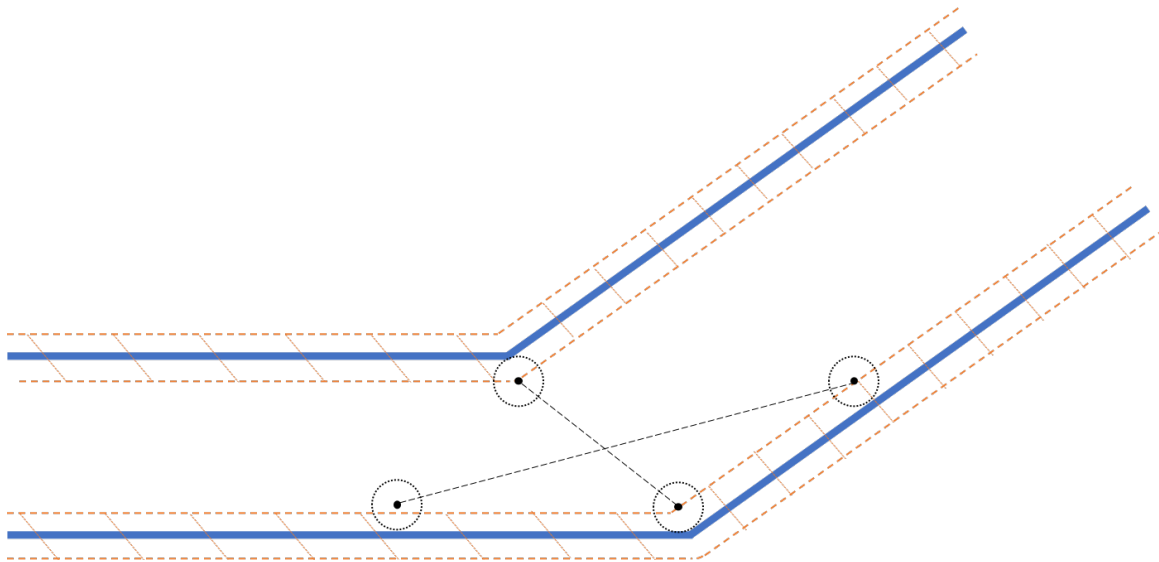


Figure 3.7: An example of a valid configuration in the geometric approach combined with the numerical approach

analysis allows for the determination of the motion path of the translating object in the case of a Prismatic-Prismatic variable joint relative to the stationary object and

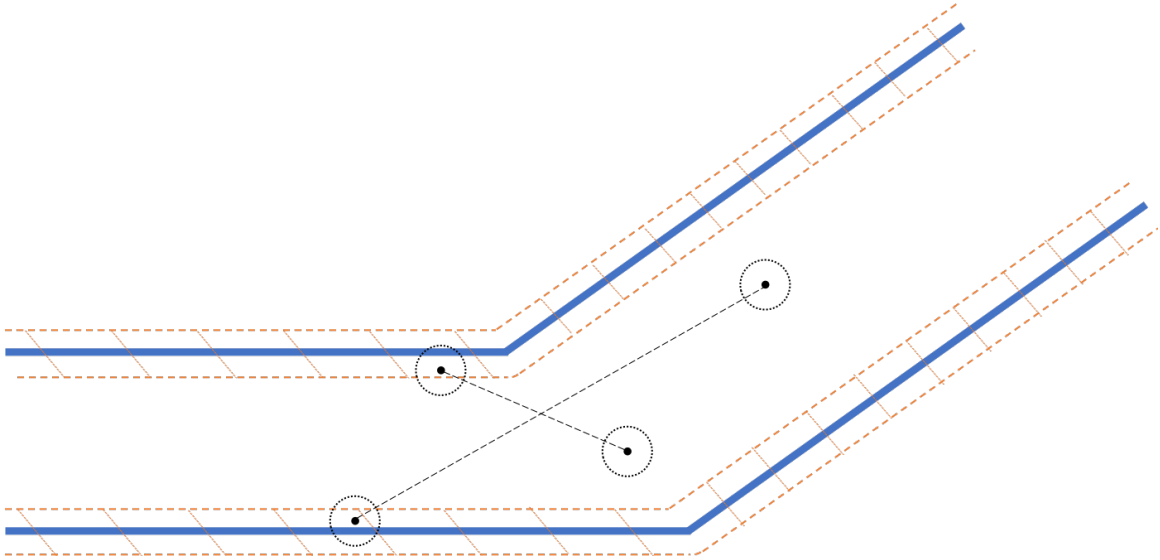


Figure 3.8: An example of an invalid configuration in the geometric approach combined with the numerical approach

thus synthesize a joint. This motion path can then be analyzed, and its limitations and restrictions can be outlined. The two approaches are important to be able to extract any potential undesired motions when the variable joints are considered with circular contacts. The two approaches will allow for Prismatic-Prismatic variable joints to be analyzed, understood, and implemented.

## CHAPTER 4

### Verification of the Synthesis of Prismatic Higher Pairs

A prismatic higher pair is a slider joint created by two objects called links, one stationary, and the other restricted to translational motion by the stationary link. This stationary link only touches each contact of the moving link at a single point, i.e., no surface contact. To be able to synthesize the motion profile of prismatic-prismatic variable joints, it is important to first validate the configuration space analysis of prismatic higher pairs before application to variable joints. Previous work analyzed various configurations of prismatic higher pairs with various numbers of contact points to determine the minimum number of contacts for each configuration.

#### 4.1 General Assumptions

Both  $P_1$  and  $P_2$  prismatic higher pairs as outlined by Slaboch [2] will be re-analyzed to validate this work as well as the methodology used. A diagram of a  $P_1$  higher pair can be seen in Figure 2.1. The rectangular link shown is assumed to be the moving link. While in actuality it can be two infinite parallel lines, it is represented as a polygon and used as the moving link to provide more intuitive results. It does

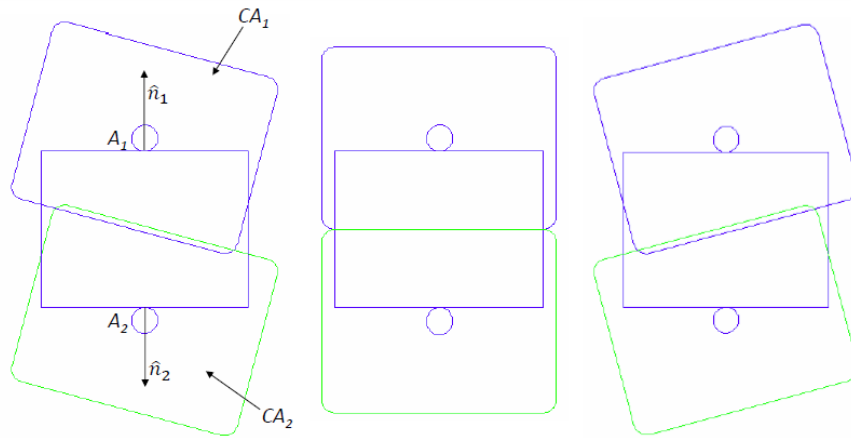


Figure 4.1: Results of Slaboch's configuration space analysis of  $P_1$  joints [2]

not matter which link is assumed to be moving because the links only need to be moving relative to each other.

The dimensions of the links are arbitrary and chosen for convenience. In these figures, the width of the rectangular moving link is 1.92 units, its height is 1.45 units and the radii of the stationary link's circle contacts are .12 units. For the  $P_1$  analysis, the contacts are centered at  $(0,.845)$  and  $(0,-.845)$ . For the  $P_2$  analysis, the contacts are centered at  $(-.4,.6)$ ,  $(.4,.6)$ , and  $(0,-.6)$ . These dimensions were chosen to best recreate Slaboch's work [2].

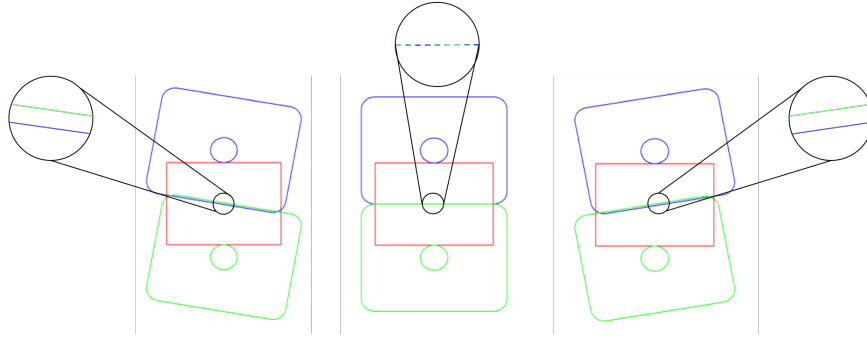


Figure 4.2: Validation of Slaboch's configuration space analysis of  $P_1$  joints

## 4.2 Configuration Space Analysis of $P_1$ Joint

A geometric approach was first taken, then confirmed with a numerical approach.

The results of Slaboch [2] are shown in Figure 4.1 which shows a prismatic joint with a rectangular moving link and two fixed stationary circular contacts to represent the fixed link. The rectangles with rounded corners are the configuration spaces of the rectangular moving link and its interaction with each stationary link's contacts.

With the rectangular link not rotated (center in Figure 4.2), there is a clear line where the configuration spaces line up without overlapping. This line is the line of motion for the moving link, showing that the joint restricts the motion to pure translation with no rotation, (i.e., a properly functioning prismatic joint).

With the rectangular moving link rotated to either  $-10^\circ$  or  $10^\circ$  (left and right in Figure 4.2), the analysis indicates an invalid configuration due to the two

configuration spaces overlapping. It indicates that the moving link would have to obstruct the stationary link's contact.

The geometric and numerical method performed in this thesis, shown in Figure 4.2, found identical results to previous research, validating both methods. When the moving link is not rotated (center), there is a clear line where the configuration spaces of each constraint coincide but do not overlap, indicating that the moving link is allowed to translate along this line. With the moving link rotated, the configuration spaces overlap, showing that it is not a valid configuration. Not only does Figure 4.2 corroborate Slaboch's analysis of  $P_1$  higher pair joints, it also serves to validate the methodologies used and outlined in Chapter 3.

### 4.3 Configuration Space Analysis of $P_2$ Joint

The procedure performed in Section 4.2, was repeated for a  $P_2$  type higher pair with the same dimensions of stationary link contacts and rectangular moving link as used for the  $P_1$ . In this pair, the translational motion is restricted by three internal contacts on the stationary link as opposed to the two external contacts of the  $P_1$ .

The results of the  $P_2$  higher pair analysis done by Slaboch is shown in Figure 4.3. Just as with the  $P_1$  joint analysis in Section 4.2, the moving link translates horizontally as designed. With the case of the  $P_2$ , when the moving link is rotated,

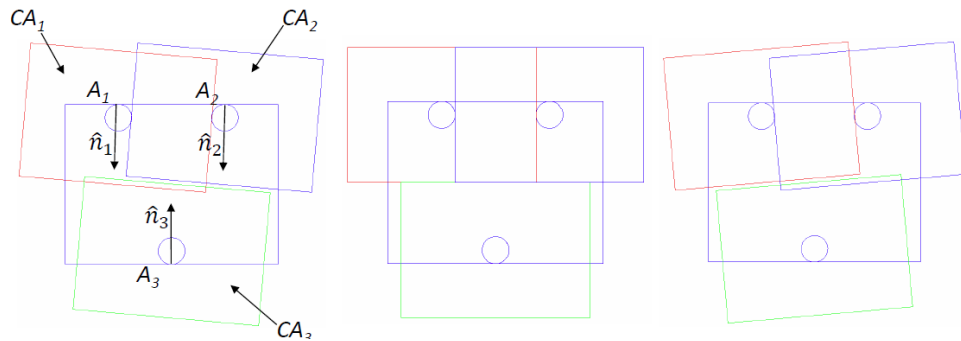


Figure 4.3: Results of Slaboch's configuration space analysis of  $P_2$  joints [2]

it loses contact with one of the stationary link. When it is rotated to  $10^\circ$  (left), the  $A_1$  and  $A_3$  contacts' configuration spaces ( $CA_1$  and  $CA_3$ ) overlap, while the  $A_2$  and  $A_3$  lose contact with each other. The moving link cannot exist at this configuration due to the overlap of the  $A_1$  and  $A_3$  configuration spaces. When the moving link is rotated to  $-10^\circ$  (right), the  $A_2$  and  $A_3$  contacts' configuration space overlap, indicating an invalid configuration.

The results using the methodology in Chapter 3 seen in Figure 4.4 show the configuration space analysis of Slaboch applied to a  $P_2$  higher pair. The results for the  $P_2$  higher pair are the same as the  $P_1$  higher pair; horizontal translation is possible at  $0^\circ$ , but two of the configuration spaces overlap at both a positive and negative rotation. Similarly to the  $P_1$  analysis of Section 4.2, the work corroborates Slaboch's work as well as validates the methodology used in this thesis.

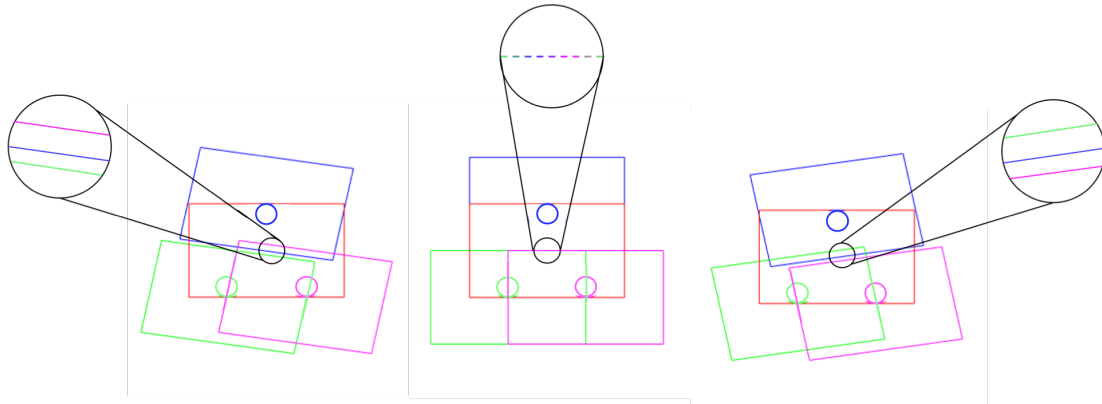


Figure 4.4: Validation of Slaboch's configuration space analysis of  $P_2$  joints

#### 4.4 Summary

Slaboch [2] used a configuration space analysis to determine the minimum number of contacts required for the stationary link to restrict the moving link to translational motion. Slaboch also analyzed these pairs with fewer contacts than the ones shown in this chapter, all of those failed, showing that Slaboch had determined the minimum number of contacts for each type of prismatic higher pair. This chapter validates this work. This information will be used in the design and analysis of Prismatic-Prismatic variable joints in Chapter 5 and 6. Also seen in this chapter, the configuration space of a circular contact and rectangle is the shape of the rectangle with rounded edges of the same radius as the circles, if the circles have no radius, the configuration space is simply the dimensions of the rectangular link.



This chapter shows the tools used for this thesis applied to previous works, ensuring the validity of the results of the methodologies discussed in Chapter 3.

## CHAPTER 5

### Prismatic-Prismatic Joint Synthesis With Point Contacts

Slaboch [2] outlined two main types of prismatic higher pairs, type  $P_1$  and type  $P_2$ . In Chapter 4, the two types of prismatic higher pairs were verified using a configuration space method. This verification defines the two types of prismatic higher pairs and their configurations. These configurations use the minimum number of contacts of a stationary link required to restrain a moving link to translational motion based on where the contact points are placed. As seen in Figure 3.5 in Chapter 3, if the stationary link's contacts are one-dimensional (i.e.,  $r = 0$ ), then the configuration space boundaries are equal to the dimensions of the moving link.

There are only three potential types of Prismatic-Prismatic variable joints:  $P_1P_1$ ,  $P_1P_2$ , and  $P_2P_2$  [2]. This chapter will demonstrate the design and limitations of each of these Prismatic-Prismatic variable joints when point contacts are utilized.

#### 5.1 Desired Motion Path

The desired motion path for a Prismatic-Prismatic Variable Joint is intuitive and easily defined. A Prismatic-Prismatic Variable joint should translate in one direction, and then another without any rotation. In Figure 5.1, a sample desired

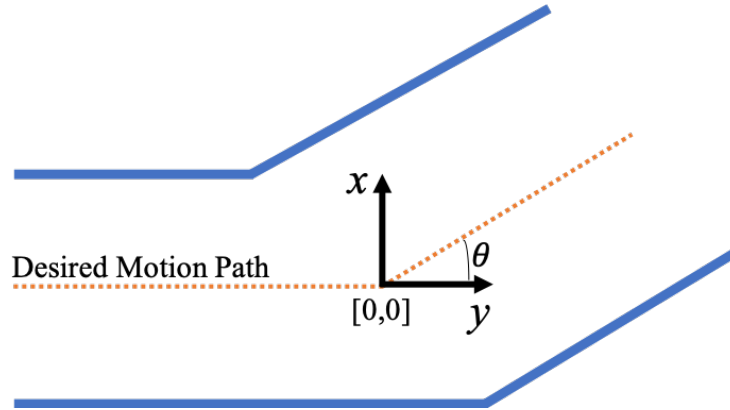


Figure 5.1: Diagram of the motion path of a Prismatic-Prismatic variable joint

motion path is shown relative to the stationary link. The desired motion path is the two lines of translation with the angle between these two lines being the desired translation angle,  $\theta$ . The center-point of transition from the one portion of the joint to the other is defined to be  $[0,0]$ .

The motion path of the moving link is:

$$q_y = \begin{cases} 0 & q_x \leq 0 \\ q_x \tan \theta & q_x > 0 \end{cases}$$

where  $q = (q_x, q_y)$  is the location of the centroid of the moving link.  $q$  is located at  $[0,0]$  when the joint transitions from one prismatic pair to another, as seen in Figure 5.1.

## 5.2 Valid and Invalid Prismatic-Prismatic Variable Joint Types

This chapter analyzes the three potential types of Prismatic-Prismatic variable joints. The analysis will be done using the geometric approach discussed in Chapter 3. This analysis is performed by defining the geometry of each of the two links, and the design dimensions that can be changed. Using the geometries of the links, it is possible to determine if the joints in question are valid by looking at the desired motion path, and determining if there are any locations at which the configuration space analysis would show it is not possible. Unlike in Chapter 4, the link with contacts will now be the moving link, and the other link consisting of lines will now be the stationary link. This notation was done to match Slaboch's work, but now with the analysis of Prismatic-Prismatic variable joints, it is important logically to view the links as they will be used, with the moving link moving and the stationary link stationary.

This chapter will use the terminology of first pairs and second pairs. The first pair is the initial prismatic higher pair as defined previously, and the second pair is the second. This can be seen more clearly in Figure 5.2. A summary of the analysis of this chapter is shown in Table 5.5. The joints feasible will have their design constraints outlined and will be further analyzed in Chapter 6 when non-ideal contacts are considered. This table shows a synthesis of

Table 5.1: Summary of analysis of various Prismatic-Prismatic variable joints with point contacts

<b>Joint Type</b>	<b>Variation</b>	<b>Validity</b>	<b>Number of Contacts</b>	<b>Redundant</b>	<b>Constraints</b>
$P_1P_1$	1	Invalid	2	No	NA
$P_1P_1$	2	Invalid	2	No	NA
$P_1P_1$	3	Valid	3	Yes	Contact coordinates outlined in Table 5.2  $\theta < 90^\circ$
$P_1P_2$	1	Invalid	5	Yes	NA
$P_1P_2$	2	Valid	5	Yes	Contact coordinates outlined in Table 5.3  $\theta < 90^\circ$
$P_2P_2$	1	Valid	4	Yes	Contact coordinates outlined in Table 5.4  Equation 5.1  $\theta < 90^\circ$

Prismatic-Prismatic variable joints, showing the different variations of

Prismatic-Prismatic variable joints and their constraints.

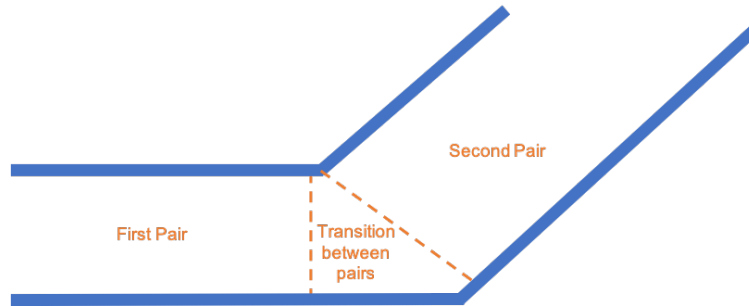


Figure 5.2: Definition of the first and second pair of a Prismatic-Prismatic variable joint

### 5.2.1 $P_1P_1$ Variable Joints

#### First Variation

Figure 5.3 shows a diagram of a potential  $P_1P_1$  joint using three moving contact points;  $c_2$  and  $c_3$  are each used for the first pair and second pair of the joint respectively, while  $c_1$  is used for both. This design ensures there are two perpendicular contacts for each prismatic higher pair, as discussed in Chapter 4. The issue with this design is that the  $c_2$  contact will keep the joint from transitioning into the second prismatic pair due to interference with the stationary link. The interference of the  $c_2$  contact and the direction of restricted motion is denoted by the arrow in Figure 5.3.

One possible change in the stationary link would be to move the transition point of the stationary link's bottom line, from the first pair to the second, which

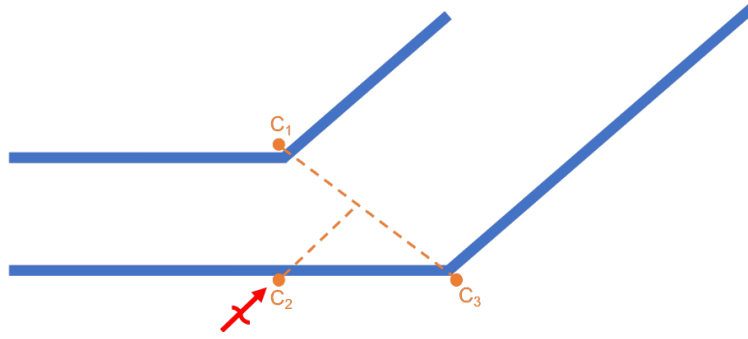


Figure 5.3: Diagram of  $P_1P_1$  first variation with point contacts and a large offset of the bottom of the stationary link

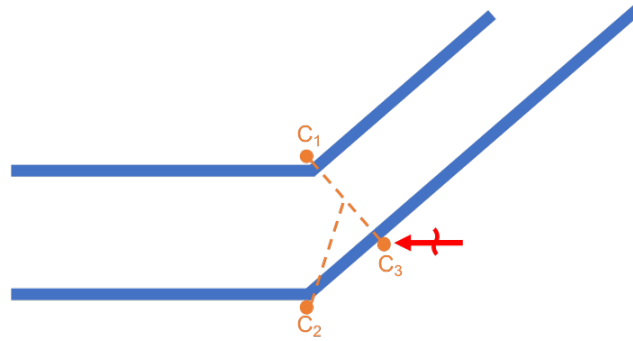


Figure 5.4: Diagram of  $P_1P_1$  first variation with point contacts and a smaller offset of the bottom of the stationary link

can be seen in Figure 5.4. While this change would enable the  $c_2$  contact to translate along the the first portion of the joint, there would then be interference with the  $c_3$  contact. The interference of the bottom right contact and the direction it is unable to move in is denoted by the red arrow in Figure 5.4.

Thus, the first variation of the  $P_1P_1$  variable joints in Figures 5.3 and 5.4 are not valid Prismatic-Prismatic variable joints.

## Second Variation

Figure 5.5 shows a diagram of a potential  $P_1P_1$  joint using two moving link contact points:  $c_1$  and  $c_2$ . The two contact points are oriented in the same configuration as in the  $P_1$  higher pair analyzed in Chapter 4. While this variation of the joint would allow for the desired motion path, it is also not a fully defined joint. The second prismatic pair of the joint allows for motions other than the desired motion path, both undesired translations and rotations. For a  $P_1$  higher pair to work, the two moving link contacts must be perpendicular to the lines of the stationary link, otherwise the moving link will be able to rotate and then translate perpendicular to the desired motion path.

To show why this design is not feasible more analytically, a configuration space analysis using the geometric method of the second prismatic pair of the joint is shown in Figure 5.6. In the second portion of the joint, the moving link is able to rotate as seen in Figure 5.6 (left) because when the link is rotated, the configuration space boundaries do not overlap. If the configuration space boundaries do not overlap, it is a valid configuration. If the configuration space when the moving link is rotated is valid, it means the link is allowed to rotate in the second pair of the joint, which is undesired. In the second variation of the  $P_1P_1$  variable joint, the two contact points do not form a line of contact perpendicular to the stationary link, resulting in an invalid joint.



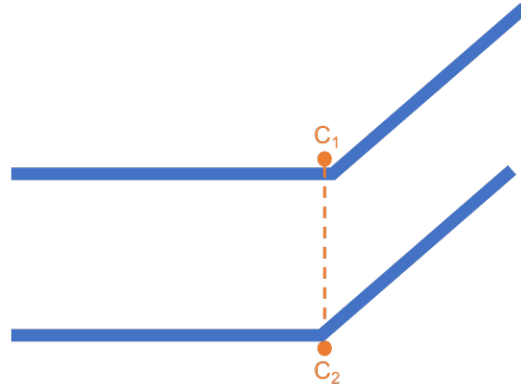


Figure 5.5: Diagram of  $P_1P_1$  second variation with point contacts

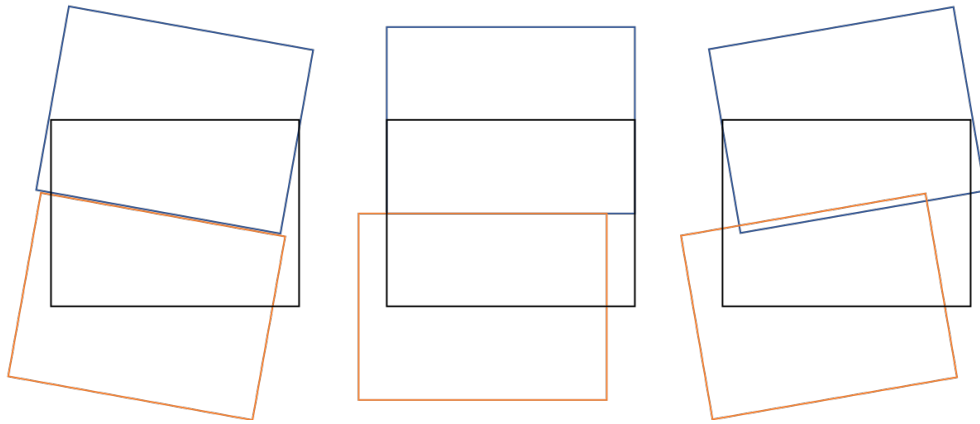


Figure 5.6: Geometric configuration space analysis of the second portion of the second variation of a  $P_1P_1$  at  $-10$  (CCW)  $^\circ$  (left),  $0^\circ$  (center), and  $10^\circ$  (CW) (right)

Thus, the second variation of the  $P_1P_1$  variable joints in Figure 5.5 is not a valid Prismatic-Prismatic variable joint.

Table 5.2: Coordinates of point contacts for moving link of a  $P_1P_1$  variable joint

	$c_1$	$c_2$	$c_3$
x	0	0	$w_{ch1}\tan(\theta)$
y	$.5w_{ch1}$	$-.5w_{ch1}$	$-.5w_{ch1}$

### Third Variation

The third variation of  $P_1P_1$  joints is valid, but contains redundancy. An example of this configuration of  $P_1P_1$  joints can be seen in Figure 5.7 with the design parameters of the moving link given in Table 5.2 where  $w_{ch1}$  is the width of the first channel and  $\theta$  is the angle of translation. It is identical to the stationary link in Figure 5.3, but with an additional stationary link line for the second prismatic pair of the joint. The moving link is then redesigned so that  $c_3$  point meets this new line of the stationary link.  $c_3$  must also form a line perpendicular to the stationary link with the  $c_1$  contact to avoid the same situation that was discussed in Figure 5.6; if the contacts are not perpendicular to the stationary link line, undesired rotations are possible. This design change allows for two contacts to be in use at a time, with both forming a normal contact line, preventing any undesired rotations.

In Figure 5.7, the third variation's contacts  $c_1$  and  $c_2$  form a prismatic higher pair for the first pair of the joint and contacts  $c_1$  and  $c_3$  form a prismatic higher pair for the second pair of the joint. Both these pairs are functional  $P_1$  higher pairs as

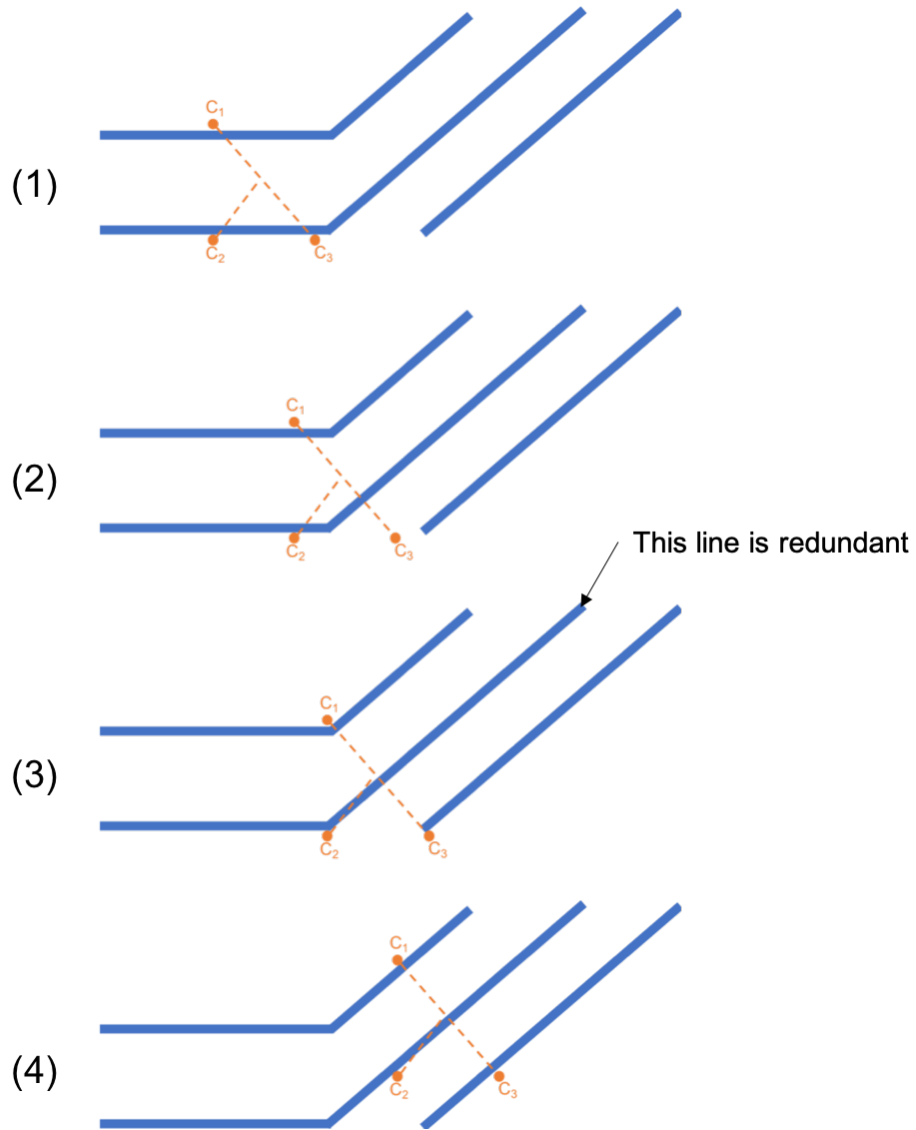


Figure 5.7: Diagram of  $P_1P_1$  third variation with point contacts shown as the moving link moves from (1) to (4)

both contacts are on the outside of the stationary joint and perpendicular to the line of motion which is required to avoid undesired rotation. But for both pairs of the joint there is a third contact that is unnecessary making this joint redundant.

Thus, Variation 3 is the only variation of  $P_1P_1$  variable joints that is valid

with the minimum number of redundancies possible. The other two variations are incapable of restricting the moving link to translational motion along the desired motion path without rotation.

### 5.2.2 $P_1P_2$ and $P_2P_1$ Variable Joints

Variable joints are designed to be able to translate in both directions transitioning to and from each higher pair of the joint. Thus, any analysis performed of a  $P_1P_2$  variable joint applies for a  $P_2P_1$  as they are simply the reverse of each other. Thus the analysis will only be done for a  $P_1P_2$ .

#### First Variation

Figure 5.3 shows a diagram of a potential  $P_1P_1$  joint using five moving contact points:  $c_1$ ,  $c_2$ ,  $c_3$ ,  $c_4$ , and  $c_5$ . The  $P_1P_2$  joint is shown using two external point contacts ( $c_1$ ,  $c_2$ ) for the first prismatic pair ( $P_1$ ), and three internal contacts ( $c_3$ ,  $c_4$ ,  $c_5$ ) for the second prismatic pair ( $P_2$ ). The design of the moving link comes from combining the  $P_1$  and  $P_2$  higher pair contacts into one.

The first variation of the  $P_1P_2$  variable joint runs into the same restriction as the first variation of the  $P_1P_1$  variable joint. As the joint transitions into the second prismatic pair of the joint, the  $c_2$  contact restricts the translation of the link due to

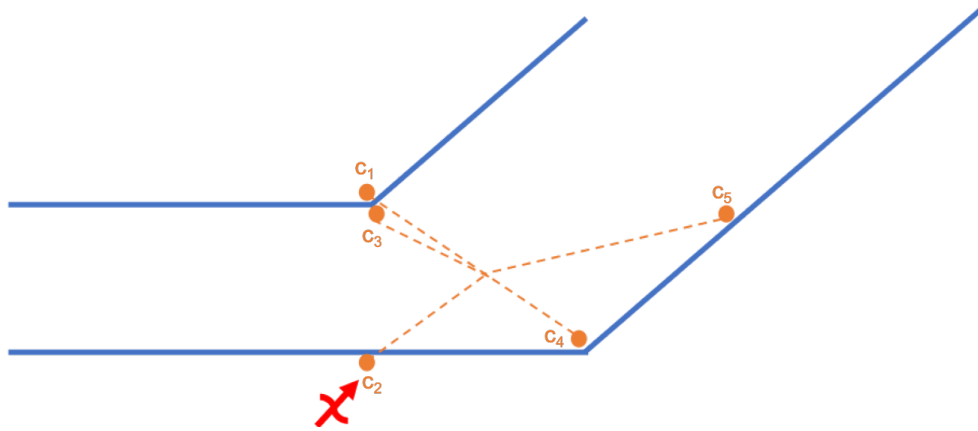


Figure 5.8: Diagram of  $P_1P_2$  with point contacts

interference with the stationary link. In Figure 5.8, the direction that the contact cannot travel is denoted with an arrow.

Thus, the first variation of the  $P_1P_2$  variable joint in Figure 5.8 is not a valid Prismatic-Prismatic variable joint.

### Second Variation

To counter the effect of the interference exhibited in Figure 5.8, the stationary link needs to be redesigned to accommodate a contiguous line. In the second variation, the transition from one prismatic pair to the other at the bottom of the stationary link is lined up with the same transition point at the top. This design allows for the moving link contact that was formerly immobilized to translate for either prismatic pair.

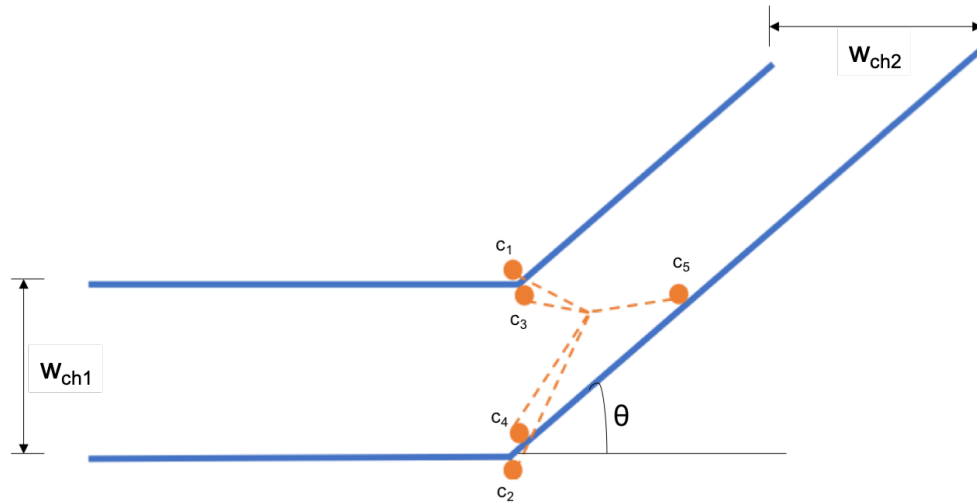


Figure 5.9: Diagram of  $P_1P_2$  with point contacts and no offset in the stationary link

The configuration shown in Figure 5.9 is a valid Prismatic-Prismatic variable joint.  $c_1$  and  $c_2$  form a  $P_1$  pair and do not interfere with the transition to the second prismatic pair.  $c_3, c_4, c_5$  form a  $P_2$  pair and do not interfere with the functioning of the first prismatic pair. However, redesigning the stationary link necessitates design constraints. The width of the second channel is directly related to the width of the first channel and the translation angle. Also translation at an angle beyond  $90^\circ$  is not possible. The design coordinates for the moving link's contacts are outlined in Table 5.3, where  $w_{ch1}$  is the width of channel 1 and  $w_{ch2}$  is the width of channel 2.

Thus, the second variation is the only variation of  $P_1P_2$  variable joints that is valid with the minimum number of redundancies possible. The other variation is

Table 5.3: Coordinates of point contacts for moving link of a  $P_1P_2$  variable joint

	$c_1$	$c_2$	$c_3$	$c_4$	$c_5$
x	0	0	0	0	$w_{ch2}$
y	$.5w_{ch1}$	$-.5w_{ch1}$	$.5w_{ch1}$	$-.5w_{ch1}$	$.5w_{ch1}$

incapable of restricting the moving link to translation motion along the desired motion path without rotation.

### 5.2.3 $P_2P_2$ Variable Joints

$P_2$  pairs require three internal constraints to retain a link to translational motion.

In Figure 5.10, a  $P_2P_2$  variable joint is designed using three internal contacts for the moving link for each portion of the joint:  $c_1$ ,  $c_2$ , and  $c_3$  for the first prismatic pair and  $c_2$ ,  $c_3$ , and  $c_4$  for the second prismatic pair. A fourth contact is required as the same three contacts cannot create a valid  $P_2$  higher pair for both prismatic pairs that make up the joint. A fourth contact point means that the joint is redundant.

There is an additional design requirement due to the required geometry of the joint; a  $P_2$  pair must have two contacts with another opposite and between them. If the desired translation angle does not meet the criteria,

$$\theta \geq \tan^{-1} \frac{w_{ch1}}{w_{ch2}}, \quad (5.1)$$

the joint will not function along the first portion as the points will not be aligned. The design requirement of Equation 5.1 is due to the single contact on one side being outside of the two contacts on the opposite side. This design requirement ensures the moving link is not able to rotate, similar to the second variation of a  $P_1P_1$  in Figure 5.5. As seen in the configuration space analysis performed in Figure 5.6, the joint will be able to rotate, which is not a desired motion. The design coordinates for the moving link's contacts are outlined in Table 5.4, where  $w_{ch1}$  is the width of channel 1 and  $w_{ch2}$  is the width of channel 2.

Thus, Variation 1 is the only variation of  $P_2P_2$  variable joints that is valid with the minimum number of redundancies possible.

Table 5.4: Coordinates of point contacts for moving link of a  $P_2P_2$  variable joint

	$c_1$	$c_2$	$c_3$	$c_4$
x	$-w_{ch1} \tan(90 - \theta) - .5w_{ch2}$	$w_{ch1} \tan(90 - \theta) - .5w_{ch2}$	$w_{ch1} \tan(90 - \theta) + .5w_{ch2}$	$-w_{ch1} \tan(90 - \theta) + .5w_{ch2}$
y	$-.5w_{ch1}$	$.5w_{ch1}$	$.5w_{ch1}$	$-.5w_{ch1}$

### 5.3 Summary

While all three types of prismatic-prismatic variable joints,  $P_1P_1$ ,  $P_1P_2$  and  $P_2P_2$ , with point contacts for the moving link, are able to be designed, they each have their own strengths and weaknesses as outlined in the Constraints column of Table 5.5. In addition, it was also found that Prismatic-Prismatic variable joints cannot



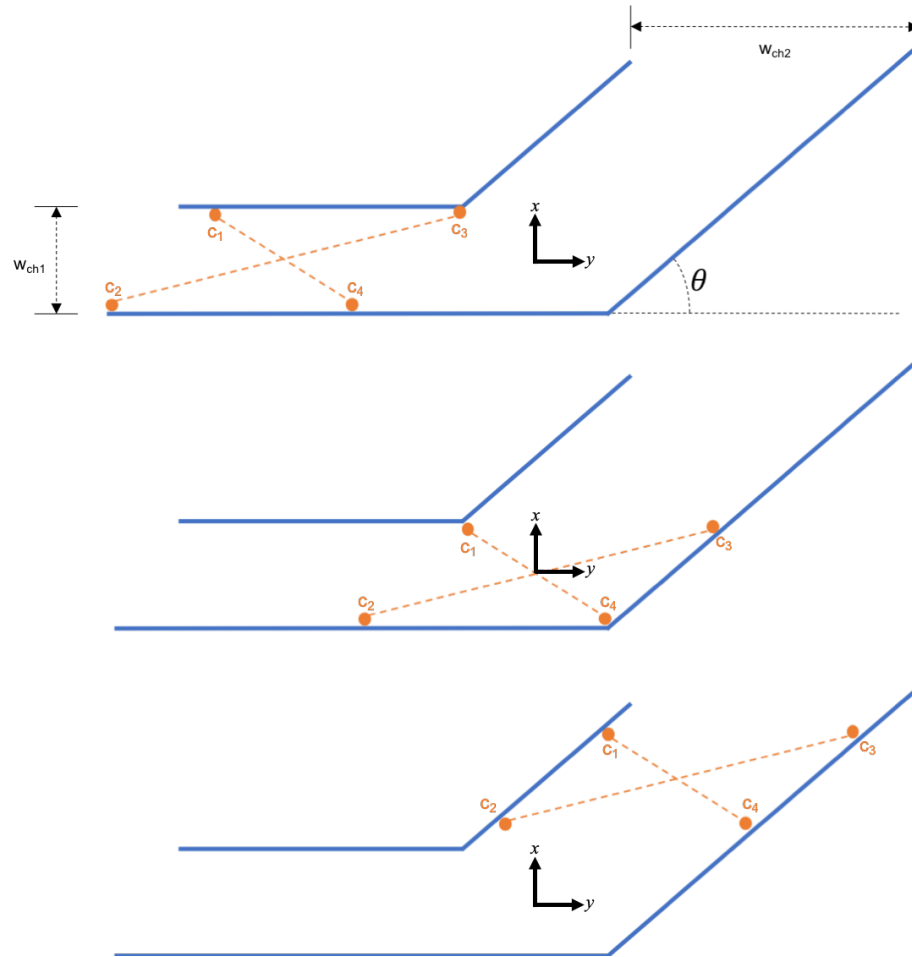


Figure 5.10: Diagram of  $P_2P_2$  with point contacts

be designed without redundant contacts. This means that these redundancies have the possibility to either make tolerances worse for joints or potentially restrict undesired motions even more depending on the joint.

Table 5.5: Summary of analysis of various Prismatic-Prismatic variable joints with point contacts

<b>Joint Type</b>	<b>Variation</b>	<b>Validity</b>	<b>Number of Contacts</b>	<b>Redundant</b>	<b>Constraints</b>
$P_1P_1$	1	Invalid	2	No	N/A
$P_1P_1$	2	Invalid	2	No	N/A
$P_1P_1$	3	Valid	3	Yes	Contact coordinates outlined in Table 5.2  $\theta < 90^\circ$
$P_1P_2$	1	Invalid	5	Yes	N/A
$P_1P_2$	2	Valid	5	Yes	Contact coordinates outlined in Table 5.3  $\theta < 90^\circ$
$P_2P_2$	1	Valid	4	Yes	Contact coordinates outlined in Table 5.4  Equation 5.1  $\theta < 90^\circ$

## CHAPTER 6

### Prismatic-Prismatic Joint Synthesis With Circular Contacts

Chapter 4 and 5 outlined and validated the two types of prismatic higher pairs,  $P_1$  and  $P_2$ , and three potential variations of Prismatic-Prismatic variable joints,  $P_1P_1$ ,  $P_1P_2$ , and  $P_2P_2$ . All potential prismatic-prismatic variable joints are possible and come with various design constraints. However, these constraints were designed for joints with one-dimensional point contacts for the moving link. In Chapter 6, these same joints will be analyzed with the contacts being more realistic circular contacts. Prismatic-Prismatic Variable Joints with circular contacts have different design and performance issues than those with one-dimensional contacts.

#### 6.1 Preliminaries

The desired motion path for a Prismatic-Prismatic variable joint is the same as the motion path defined in Chapter 4. In this chapter, the contacts will be analyzed as two-dimensional circular contacts which can cause a variation from this ideal motion path, both in translation and rotation. For this reason, the numerical approach outlined in Chapter 3 will be used to analyze this undesired motion.

## 6.2 Valid and Invalid Prismatic-Prismatic Variable Joint Types

Table 6.1 shows the conclusions from the various types of Prismatic-Prismatic variable joints including the constraints caused by the moving links consisting of circular contacts. This table allows the reader a map to the chapter and a complete summary of the contributions made in this chapter.

### 6.2.1 $P_1P_1$ Variable Joints

#### First Variation

It was determined in Chapter 5 that this variation is not possible with point contacts. Thus, it is also not possible with circular contacts.

#### Second Variation

It was determined in Chapter 5 that this variation is not possible with point contacts. Thus, it is also not possible with circular contacts.

Table 6.1: Summary of analysis of various Prismatic-Prismatic variable joints with circular contacts

Joint Type	Variation	Validity	Number of Contacts	Redundant	Constraints
$P_1P_1$	1	Invalid	2	No	N/A
$P_1P_1$	2	Invalid	2	No	N/A
$P_1P_1$	3	Valid	3	Yes	Contact coordinates outlined in Table 5.2  Figure 6.5  $\theta < 90^\circ$
$P_1P_2$	1	Invalid	5	Yes	N/A
$P_1P_2$	2	Valid	5	Yes	Contact coordinates outlined in Table 5.3  $\theta < 90^\circ$
$P_2P_2$	1	Valid	4	Yes	Contact coordinates outlined in Table 5.4  Equation 5.1  Figure 6.5  $\theta < 90^\circ$

### Third Variation

To allow for a  $P_1P_1$  joint to function using circular contacts, both links must be redesigned. The centers of the point contacts must be offset from the stationary link by the radius of the circular contacts. The stationary link must also be redesigned

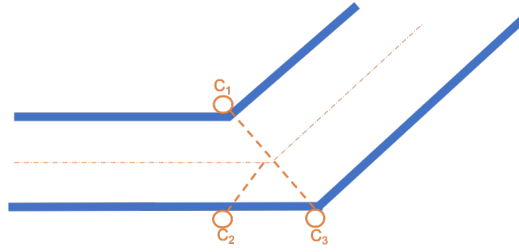


Figure 6.1: Diagram of  $P_1P_1$  with circular contacts and no offset

to accommodate circular contacts. The bottom line of the stationary link must be offset by

$$Offset_{StationaryLink} = r_{contact} \cos(\theta) \quad (6.1)$$

where  $r_{contact}$  is the radius of the contacts and  $\theta$  is the desired translation angle.

This offset is to ensure the bottom circular contact is able to translate when the link transitions over to the second prismatic pair of the joint. A  $P_1P_1$  joint with no offset can be seen in Figure 6.1 and an example of the same joint with an offset can be seen in Figure 6.2. An offset designed into the stationary link is necessary, but then enables for the moving link to have a small amount of undesired rotation.

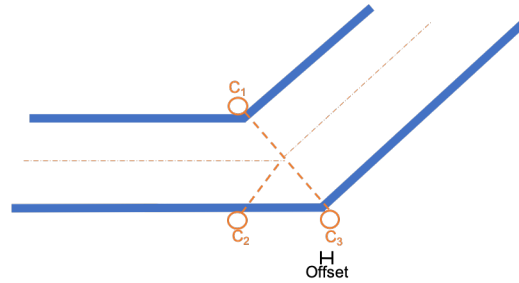


Figure 6.2: Diagram of  $P_1P_1$  with circular contacts and an offset

### 6.2.2 $P_1P_2$ and $P_2P_1$ Variable Joints

#### First Variation

It was determined in Chapter 5 that this variation is not possible with point contacts. Thus, it is also not possible with circular contacts.

#### Second Variation

The point contact design for a  $P_1P_2$  variable joint was synthesized in Chapter 5, but there are additional design considerations when the moving link has circular contacts. The design considerations for a stationary link for a  $P_1P_2$  variable joint are similar to that of a  $P_1P_1$ . An offset needs to be designed into the stationary link to allow the circular constraint to translate.

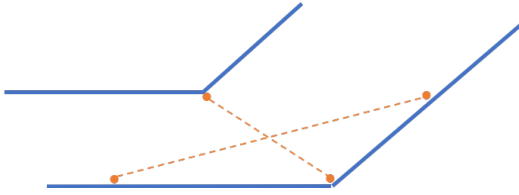


Figure 6.3: Sample  $P_2P_2$  with point contacts

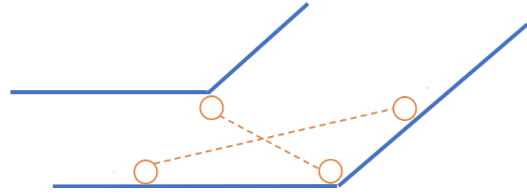


Figure 6.4: Sample  $P_2P_2$  with circular contacts

### 6.2.3 $P_2P_2$ Variable Joints

Similarly to  $P_1P_2$  and  $P_1P_1$  joints, the  $P_2P_2$  joint needs to be redesigned to accommodate the circular contacts to be valid. Unlike the  $P_1P_2$  joint, the  $P_2P_2$  joint only requires a redesign of the moving link. In this case, the moving link contact's centers need to be spaced one radius from the stationary link vertically. The redesign of the link can be seen in Figures 6.3 and 6.4.

## 6.3 Numerical Analysis of Prismatic-Prismatic Variable Joints

Due to the use of circular contacts in this chapter, the configuration space analysis must be performed using the numerical approach outlined in Chapter 3. This approach analyzes the various poses at which the moving link can exist in relation to the stationary link that vary from the ideal motion path in the form of undesired rotations. In particular, all three types of Prismatic-Prismatic variable joints will be analyzed to determine if the moving link is able to rotate and the effects of various



design variables on this rotation. In particular, the analysis in this section is done at the transition point between the two prismatic pairs as this is the part of the joint allows for the circular contacts to cause undesired rotation.

### 6.3.1 $P_1P_1$ Variable Joints

The numerical method described in Chapter 3 determined that the moving link of  $P_1P_1$  variable joints with circular contacts is able to have undesired rotation. Figure 6.6 shows the configuration space of a  $P_2P_2$  joint in the  $x$  and  $\psi$  plane where  $x$  is the horizontal direction and  $\psi$  is the undesired rotation of the moving link. Figure 6.7 shows the maximum rotation of the moving link with respect to  $x$ . The maximum rotation of the moving link is the standard by which a joint's performance is determined.

For a  $P_1P_1$  variable joint, there are two design parameters that need to be considered when determining how susceptible the joint is to undesired rotations: circular contact radius and translation angle. The ratio of the sizes of the channels do not need to be taken into consideration as the ratio is dependent on the translation angle. Because changes in the contact radius and translation angle both effect the undesired rotation of the moving link, it is important to analyze how they interact. For this reason, the maximum undesired rotation extracted from the numerical analysis is presented in a designed experiment shown in Figure 6.5. The

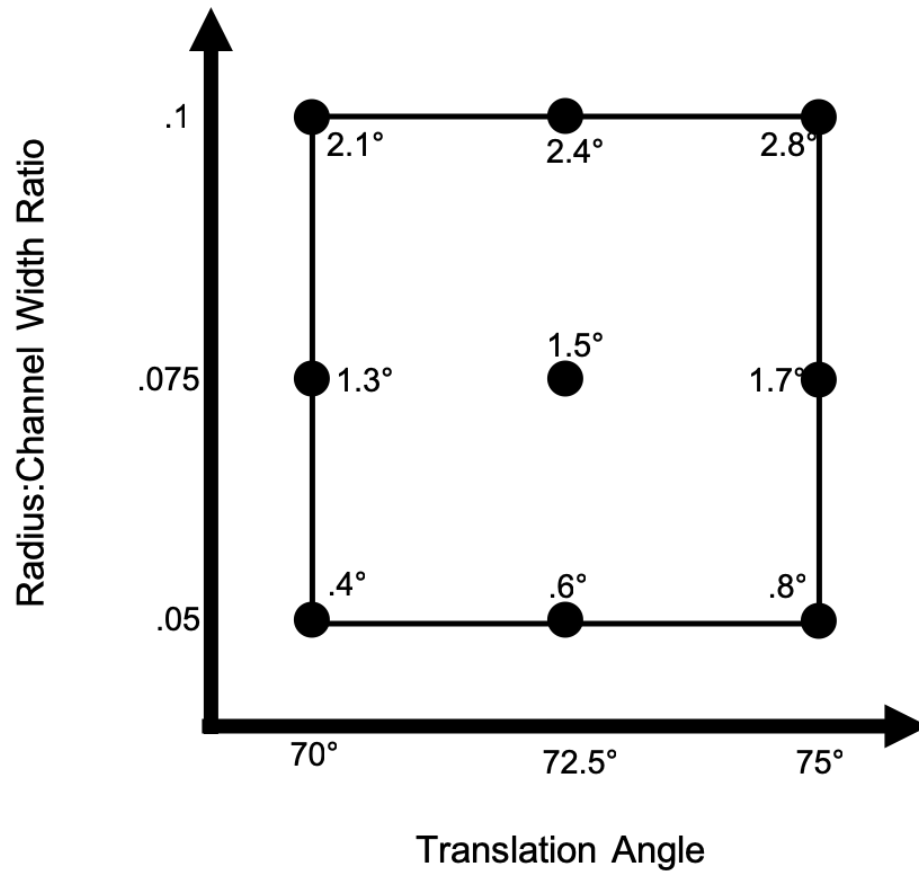


Figure 6.5: Maximum undesired rotations of  $P_1P_1$  joints with respect to changes in contact radius and translation angle

ranges represented in Figure 6.5 were chosen as they show the range at which the greatest undesired rotation happen.

Figure 6.5 shows that while translation angle has an important impact on the potential for the moving link to rotate, it does not have as big of an impact as the radius of the circular contacts for the range analyzed. The radius of the contacts

have a greater impact than the translation angle because their size is the direct cause of the undesired rotations of the moving link.

### **6.3.2 $P_1P_2$ Variable Joints**

After using the numerical method described in Chapter 3, it was determined that the moving link of  $P_1P_2$  variable joints with circular contacts do not have undesired rotation. Although the design of the joint needs to be different from the point contact case, the resulting joint geometry results in a joint with zero undesired rotation. The lack of undesired rotation of the moving link is an advantage of this type of Prismatic-Prismatic variable joint and should be taken into consideration when implementing these joints into reconfigurable mechanisms.

### **6.3.3 $P_2P_2$ Variable Joints**

Unlike the  $P_1P_2$  joint, the  $P_2P_2$  joint is highly susceptible to undesired rotation of the moving link when circular contacts are used. This undesired rotation is due to the way the points need to be aligned to restrict both portions to translational motion. For a  $P_2P_2$  variable joint, all of the contacts are internal. Thus, unlike with the  $P_1P_2$  variable joint, there is no additional external contact to restrict undesired rotation. There is also less restriction on undesired translational deviations from the

desired motion path, which can be seen with the joint geometry, and through a configuration space analysis.

Figures 6.6 through 6.7 show an example the results of a configuration space analysis of a  $P_2P_2$  variable joint with circular contacts. The joint in this analysis has a translation angle of  $75^\circ$ , channel width of 1 unit for each portion of the joint, and a contact radius of .1 units.

Figure 6.7 shows the maximum potential rotations of the moving link of a  $P_2P_2$  joint as a function of horizontal movement. This analysis is repeated and analyzed while varying aspects of the joint design to determine the impact of these aspects on the performance of the joint.

Similar to Figure 6.5 for a  $P_1P_1$  variable joint, a parametric study for a  $P_2P_2$  variable joint, is presented in a design of experiment format in Figure 6.8. The design of experiment format allows for all of the factors that contribute to undesired rotation be examines as a whole.

The radius of the contacts for a  $P_2P_2$  variable joint relates to the deviation of the moving link from the ideal motion path. As seen in Figure 6.8, contact radius has the largest effect on undesired rotation for a  $P_2P_2$ , for the range studied. While both the channel width ratio and translation angle have an impact on the ability for the moving link to rotate, they are less impactful compared to contact radius for the

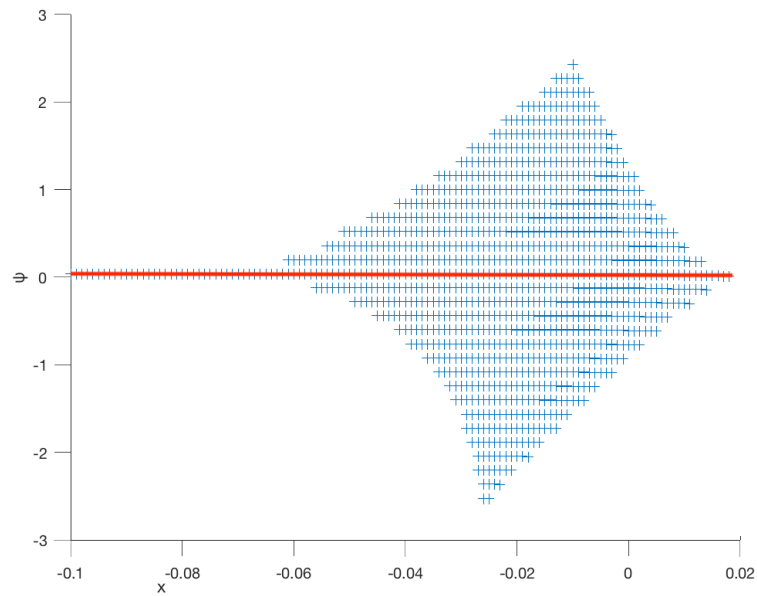


Figure 6.6: Configuration space of a  $P_2P_2$  in the  $x$  and  $\psi$  directions. The blue is the potential configurations, the red is the desired motion path

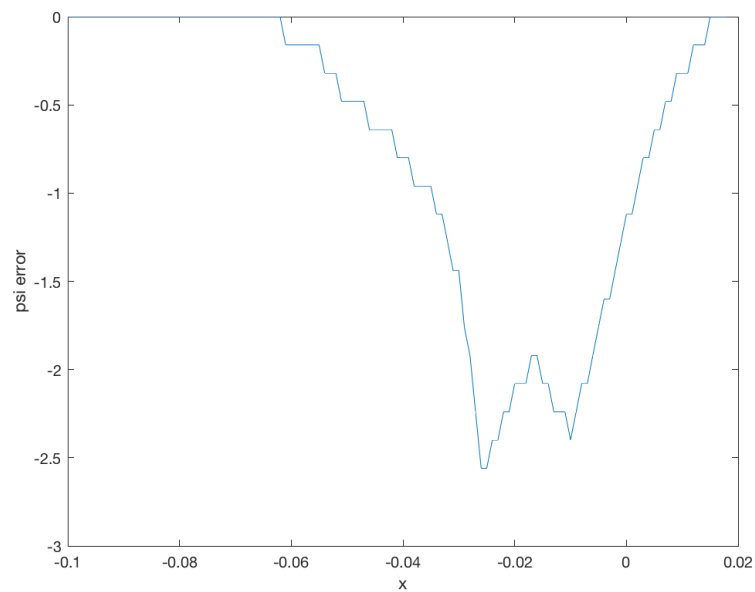


Figure 6.7: The maximum  $\psi$  error from the desired motion path for each corresponding  $x$

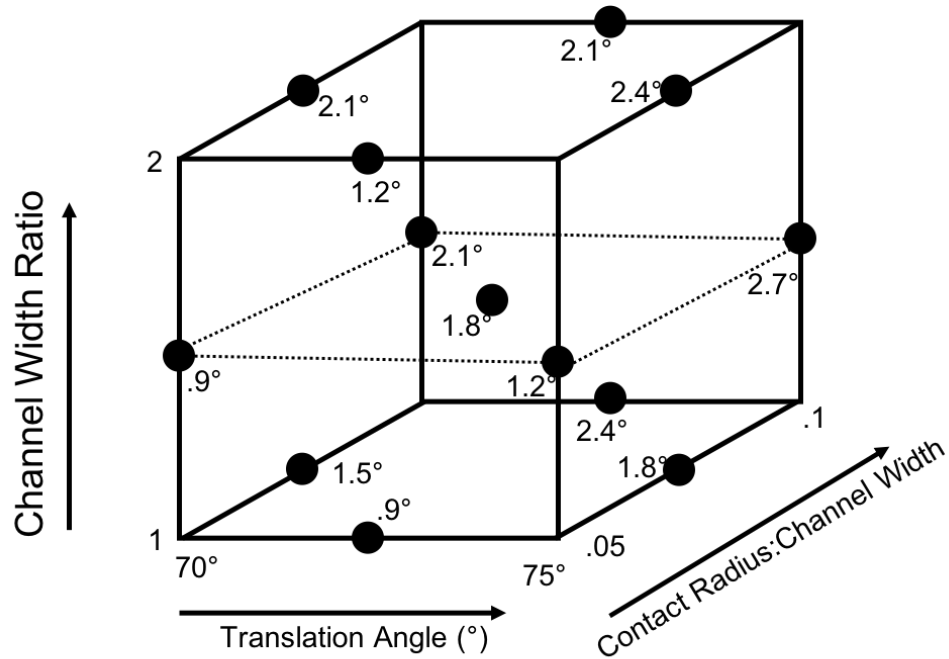


Figure 6.8: Maximum undesired rotations of a  $P_2P_2$  variable joint with respect to various factors.

values shown. Contact radius being the biggest factor on undesired rotations of the joint makes sense, as it is the direct cause of the rotation. As seen in Chapter 5, when the contact radius is 0 (contacts are point contacts) there are no undesired rotations. Translation angle is dependent on the application and is not a design choice, unlike the channel width ratio.

## 6.4 Comparison of Prismatic-Prismatic Variable Joints

The analysis of  $P_1P_1$ ,  $P_1P_2$ , and  $P_2P_2$  variable joints illustrates that there is no perfect design. The design is impacted by the ability to minimize the contact radius of the moving link, and the desired translation angle and the ratio of the widths of the stationary link's channels. It is important to clearly compare the three joints and the constraints that come with them to properly implement the joints based on a mechanism's requirements.

$P_2P_2$  variable joints with or without circular contacts are subject to the limitation on translation as defined by Equation 5.1, which is a ratio of the widths of the channels to ensure that the contacts form a triangle for each prismatic pair.  $P_1P_2$  and  $P_1P_1$  are not subject to this same limitation. Technically,  $P_1P_2$  variable joints and  $P_1P_1$  variable joints are limited only by

$$\theta_{P_1P_1} < 90^\circ \tag{6.2}$$

and

$$\theta_{P_1P_2} < 90^\circ. \tag{6.3}$$

The ratio of the channel widths of a  $P_2P_2$  joint are defined in Equation 5.1 and the ratio of the channel widths of a  $P_1P_2$  and  $P_1P_1$  are defined by Equation 6.4. These constraints limit the ability of the engineer to design the joint to the specification

required by the mechanism. These limitations are especially true once the dynamics of the joint are considered. If the ratio of channel widths needs to be small as defined by

$$\frac{w_{ch1}}{w_{ch2}} = \sin^{-1}(90 - \theta), \quad (6.4)$$

the one channel becomes over-sized as needed to handle the forces just so the second channel is capable of handling the loads required. Such a design would lead to an over-sized joint for the application and an important consideration when selecting a joint.

Another design requirement of the joint comes with the offset between the two lines of the stationary link as seen on a  $P_1P_2$  joint in Figure 6.2. For a  $P_1P_1$  or  $P_1P_2$  joint, this offset is defined by Equation 6.5. While this consideration is important when designing the stationary link, it has little impact on joint selection for a mechanism. The offset of the stationary link,

$$Offset_{Link2} = w_{ch2} \cos(90 - \theta) \quad (6.5)$$

is not a design advantage or disadvantage for either type of Prismatic-Prismatic variable joint but must be considered.



## 6.5 Summary

Each type of Prismatic-Prismatic variable joints comes with its own design considerations and constraints.  $P_2P_2$  joints are highly susceptible to undesired rotational and translational motions when the moving link's contacts are assumed to be circular, where  $P_1P_2$  joints are not. Also,  $P_1P_2$  and  $P_1P_1$  joints are able to translate at shallow angles (i.e.,  $\theta < 20^\circ$ ) much more easily than  $P_2P_2$  joints.

Understanding how the various joint design aspects impact the moving link's ability to rotate will inform engineers on the design disadvantages of these joints, especially when considering the dynamic forces within the joint, and material choice when considering the frictional forces that may result in the joint jamming. The constraints outlined in this chapter are purely kinematic; a dynamic analysis would include these limitations in addition to others. An example being that while a  $P_2P_2$  joint is valid below  $90^\circ$ , the slightest deflection would break the joint if it is near  $90^\circ$ .

## CHAPTER 7

### Potential of a Revolute-Prismatic-Prismatic Variable Joint

With the joints developed in this thesis, there is a potential for Revolute-Prismatic and Prismatic-Prismatic variable joints to be combined into a Revolute-Prismatic-Prismatic variable joint. Slaboch [2] outlined six types of Revolute-Prismatic variable joints, with both  $P_1$  and  $P_2$  higher pairs for the Prismatic portion of the joint. All three Prismatic-Prismatic variable joint will be analyzed in combination with a Revolute-Prismatic joint to determine if they are possible to be used in a Revolute-Prismatic-Prismatic variable joint.

#### 7.1 $R_nP_1P_1$ Joints

With the design of the translating link of a  $P_1P_1$ , it is not possible for the link to be rotated into position by a revolute pair. As shown in Figure 7.1, contact  $c_3$  interferes with the stationary link and is unable to get into position. As the link transitions from an Revolute-Prismatic to a Prismatic-Prismatic joint,  $c_3$  interferes with the stationary link and is unable to allow the translating link to get into the proper position. Thus,  $R_nP_1P_1$  variable joints are not possible.

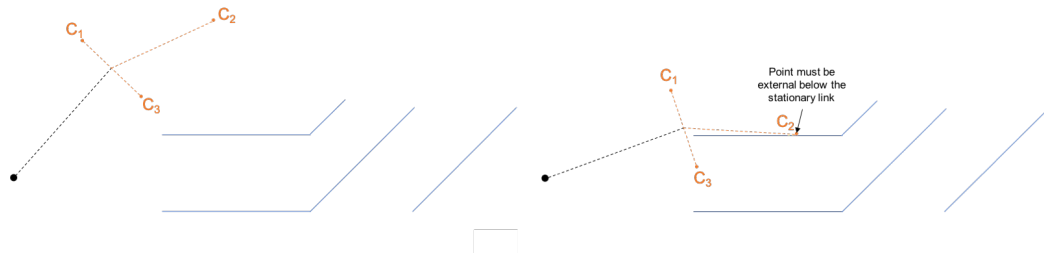


Figure 7.1: Analysis of a  $P_1P_1$  variable joint with a Revolute pair

## 7.2 $R_nP_1P_2$ Joints

Any possible  $R_nP_1P_2$  joints are subject to the design considerations and constraints of a  $P_1P_2$  variable joints. Due to the design of the translating link of  $P_1P_2$  joints outlined in Chapter 5, it is not possible for a  $R_nP_1P_2$  joint to exist. As the joint rotates in the revolute portion and approaches the transition to the first prismatic portion, the contacts for the  $P_2$  portion of the joint will interfere with the stationary link of the joint, as shown in Figure 7.2. The contact  $c_5$  of the  $P_2$  higher pair is unable to become internal to the stationary link, keeping the joint from properly transitioning to the  $P_1$  higher pair of the joint. Thus,  $R_nP_1P_2$  joints are not possible.

## 7.3 $R_nP_2P_2$ Joints

A  $R_nP_2P_2$  is technically possible to exist, but there is a significant portion of the joint where the moving link is not constrained to the desired motion. Because the

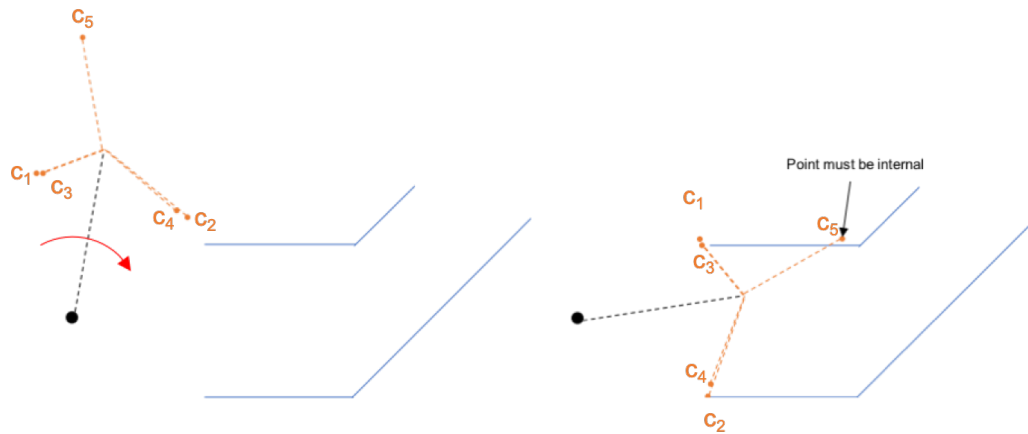


Figure 7.2: Diagram showing the interference caused by a  $R_n P_1 P_2$  joint

moving link is not properly constrained, the link is effectively invalid. The stationary link needs to be designed to accommodate the rotation of the moving link. Specifically, the length of the upper line of the stationary link,  $l_1$  needs to be shorter than the length of the lower line,  $l_2$ , by the relationship

$$l_2 - l_1 = w_{ch1} \sin \theta \quad (7.1)$$

where  $l_1$  and  $l_2$  are the lengths of the stationary link for the first prismatic pair and  $w_{ch1}$  is the width of the channel. As the joint rotates to allow for the first portion of translational motion, only two moving link contact points are in contact with the stationary link, which can be seen in Figure 7.3. In Chapter 4, it was noted that a  $P_2$  higher pair requires three contact points to restrict a link to translational

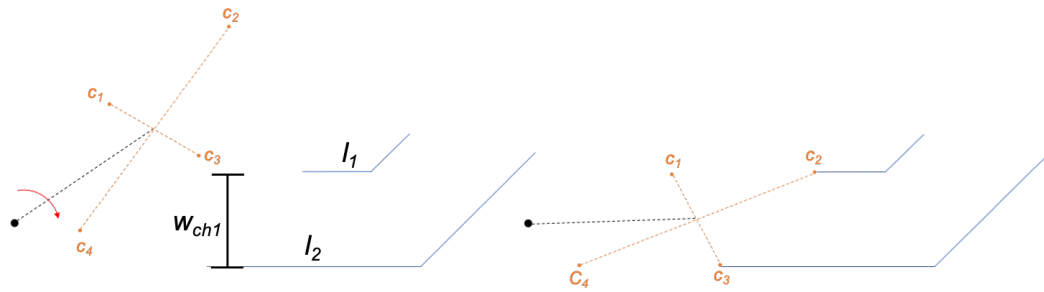


Figure 7.3: Diagram of a  $R_n P_2 P_2$  joint, showing the two contact points available for the initial prismatic motion

motion. For this reason, until the moving link translates to allow  $c_1$  to make contact with the stationary link, the moving link is able to rotate.

A configuration space analysis shows that after the link has rotated, it is also able to translate in the  $y$  direction due to only two of the three contacts necessary for a  $P_2$  higher pair. Because of this undesired rotation and translation,  $R_n P_2 P_2$  is not a feasible design for a Revolute-Prismatic-Prismatic variable joint.

#### 7.4 Summary

$R_n P_1 P_2$  variable joints are impossible to be designed due to interference of the moving link with the stationary link. While the desired motion path of a  $R_n P_2 P_2$  variable joint is possible, numerous other motion paths are also available to the moving link, meaning the joint is not functional. Using the research performed by Slaboch [2] in combination with the synthesis performed in Chapter 5,

Revolute-Prismatic-Prismatic variable joints are not possible under the assumptions of this thesis.

## CHAPTER 8

### Summary and Future Work

This thesis has provided the design requirements of the synthesis of Prismatic-Prismatic variable joints. The understanding of these design requirements allow for engineers to design Prismatic-Prismatic variable joints which can be used in Type II Mechanisms with Variable Topology. Three types of Prismatic-Prismatic variable joints are possible and outlined:  $P_1P_1$ ,  $P_1P_2$  and  $P_2P_2$ . These joints have their own design considerations and constraints, especially when designing them with circular contacts. The advantages and disadvantages of each joint are outlined completing a complete and thorough synthesis of Prismatic-Prismatic variable joints.

#### 8.1 Contributions

Chapter 5 uses a geometric approach to determine the validity of various Prismatic-Prismatic variable joints. Because there are two forms of prismatic higher pairs, there are three combinations of potential Prismatic-Prismatic variable joints. The design constraints of  $P_1P_2$  and  $P_2P_2$  are defined via a thorough synthesis of these joints. This synthesis is a contribution that has never been performed and enables the design and implementation of Prismatic-Prismatic variable joints. The

ultimate goal of this research is to allow for Prismatic-Prismatic variable joints to be selected and implemented into reconfigurable mechanisms. Implementing these joints would not be possible without the design constraints defined in this thesis.

While the work of Chapter 5 will allow for Prismatic-Prismatic variable joints to be implemented into reconfigurable mechanisms, Chapter 6 serves to provide the same tools while assuming the joints use circular two-dimensional contacts. For practical purposes, one-dimensional objects do not exist. When manufacturing variable joints in real world applications, it is important to understand the effect of imperfect manufacturing processes that may lead to non-ideal contacts. A direct comparison of the two types of Prismatic-Prismatic variable joints and how they are able to handle non-ideal contacts was presented. This information will allow for engineers to properly select and implement these joints.

## 8.2 Future Work

There are 21 possible variable joints while only 2 ( $R_nP_m$ ) have been synthesized up until this point. As more variable joints are synthesized, the opportunities for reconfigurable mechanisms greatly expands as well. With more variable joints, engineers will be able to be more creative in the design of reconfigurable mechanisms, not only pushing the field of reconfigurable mechanisms forward, but provides all of the benefits that comes with reconfigurable mechanisms.



While this thesis has helped in the design of reconfigurable mechanisms, there is still a considerable amount of work to be done. There are two main opportunities that should be tackled next with this work. First would be a quasi-static analysis of Prismatic-Prismatic variable joints to consider links with dynamic forces as there would be in real life. As an example, when  $P_2P_2$  variable joints approach 90 degrees, while they would be valid in a rigid body situation, the slightest flex of either of the links would allow the moving link to slip out of place and break the joint. Understanding how these joints can be driven and react under dynamic load would be the logical next step in this research.

The second opportunity would be to look at Prismatic-Prismatic variable joints with non-circular two-dimensional contacts. This would allow for unique designs that would mitigate the undesired motions seen in Chapter 6 and better optimize Prismatic-Prismatic variable joints. Examples of shapes that could reduce the undesired rotations would be triangles or crescents. Analyzing Prismatic-Prismatic variable joints or any variable joints with various two-dimensional shapes could be key to unlocking their potential. Different shapes may be able to bridge the gap of realistic two-dimensional design while minimizing the design constraints outlined in Chapters 5 and 6. This thesis, specifically Chapter 6, outlines the procedure for analyzing these various different shapes and

their impact on undesired rotations, allowing for research to happen rapidly, advancing the field.

This thesis lays the foundation for future work to further advance the field of variable joints. Chapter 5 is a synthesis of Prismatic-Prismatic variable joints and defines their design and limitations. Chapter 6 goes a step further and analyzes Prismatic-Prismatic variable joints with circular contacts. The methodology outlined in Chapter 6 will allow for future synthesis of variable joints with two-dimensional contact points to be done. Chapter 7 also provided a framework for analyzing variable joints with three or more higher pairs. The work in this thesis provides tools and insights into Prismatic-Prismatic variable joints but in addition it outlined methodologies for numerous future advancements in the design, synthesis, and implementation of variable joints.

## References

- [1] A.Kennedy, *The Mechanics of Machinery*. London: MacMillan and Co., 1886.
- [2] B.Slaboch, “Profile synthesis of planar variable joints,” Ph.D. Thesis, Marquette University, 2013.
- [3] A. Buchta, “The kinematic synthesis of a planar mechanism with variable topology based on a qualitative survey,” Master’s thesis, Marquette University, 2018.
- [4] J. Dai and J. Jones, “Matrix representation of topological changes in metamorphic mechanisms,” *Journal of Mechanical Design*, vol. 127, pp. 837–840, July 2005.
- [5] C. Kuo, “Structural characteristics of mechanisms with variable topologies taking into account the configuration singularity,” Master’s thesis, National Cheng Kung University, 2004.
- [6] Z. Lan and R. Du, “Representation of topological changes in metamorphic mechanisms with matrices of the same dimension,” *Journal of Mechanical Design*, vol. 130, July 2008.
- [7] J. Latombe, *Robot Motion Planning*. Kluwer, 2010.
- [8] P. Malak, “Analysis and synthesis of a planar reconfigurable mechanism with a variable joint,” Master’s thesis, Marquette University, 2016.
- [9] F. Reuleaux and A. Kennedy, *Kinematics of Machinery*. Macmillan, 1876.
- [10] E. Rimon and J. Burdick, “A configuration space analysis of bodies in contact - 1st order mobility,” *Machine Theory*, vol. 30, no. 6, pp. 897–912, 1995.
- [11] —, “A configuration space analysis of bodies in contact - 2nd order mobility,” *Machine Theory*, vol. 30, no. 6, pp. 913–928, 1995.
- [12] E. Sacks and L. Joskowicz, *The Configuration Space Method for Kinematic Design of Mechanisms*. MIT, 2010.
- [13] B. Slaboch and P. Voglewede, “Mechanism state matrices for planar

- reconfigurable mechanisms,” in *Journal of Mechanisms and Robotics*, ser. 1, vol. 3. American Society of Mechanical Engineers, February 2011.
- [14] L. Tsai, *Mechanism Design - Enumeration of Kinematic Structures According to Function*. CRC, 2001.
- [15] F. S. W. Shieh and D. Chen, “On the topological representation and compatibility of variable topology mechanisms,” in *ASME Design Engineering Technical Conference*, vol. 7. American Society of Mechanical Engineers, September 2009, pp. 1223–1230.
- [16] K. Waldron, “The constraint analysis of mechanisms,” *Journal of Mechanisms*, vol. 1, no. 2, pp. 101–114, 1966.
- [17] —, “A method of studying joint geometry,” *Mechanism and Machine Theory*, vol. 7, no. 3, pp. 347–353, 1972.
- [18] K. Wohlhart, *Kinematotropic Linkages*. Kluwer Academic, 1996.
- [19] H. Yan and C. Kuo, “Topological representations and characteristics of variable kinematic joints,” *Journal of Mechanical Design*, vol. 128, pp. 384–391, March 2006.

## APPENDIX A

### Matlab Code

#### A.1 Geometric Analysis of Higher Pairs and Variable Joints

This Matlab program allows for the configuration space analysis of higher pairs and variable joints via a geometric methodology.

```

1 clear all
2 clc
3 %% Inputs
4 n_circle = 100;
5 ch1 = 10;
6 ch2 = 20;
7 theta = 40;
8
9
10 initial_center = [0;0];
11 initial_radius = 0;
12
13 circle_1.center = [ch1;ch1+initial_radius];
14 circle_2.center = [-.2*ch1;-initial_radius];
15 circle_3.center = [ch1+ch2+2.81*initial_radius;ch1+initial_radius];
16 circle_4.center = [1.52*ch1+ch2*initial_radius;0];
17
18 thetaR = deg2rad(theta);
19 corner_bl.center = [initial_center(1);initial_center(2)];
20 corner_ul.center = ...
    [initial_center(1)+ch1/tan(thetaR);initial_center(2)+ch1];
21 corner_ur.center = ...
    [initial_center(1)+ch1/tan(thetaR)+ch2;initial_center(2)+ch1];
22 corner_lr.center = [initial_center(1)+ch2;initial_center(2)];
23
24 %% Creating Initial C.S.
25 t = 1.5*pi;
26 i = 1;
27 n=1;
28 while i <= n_circle
29     x_1 = initial_radius * cos(t);
30     y_1 = initial_radius * sin(t);
31     s_prime(1,n) = x_1 + corner_bl.center(1);
32     s_prime(2,n) = y_1 + corner_bl.center(2);
33     t = t - (.5*pi+thetaR)/n_circle;
34     i = i+1;
35     if n == 1
36         start = s_prime;
37     end
38     n=n+1;
39 end
40 i=0;
41 while i <= n_circle
42     x_1 = initial_radius * cos(t);
43     y_1 = initial_radius * sin(t);
44     s_prime(1,n) = x_1 + corner_ul.center(1);
45     s_prime(2,n) = y_1 + corner_ul.center(2);
46     t = t - (.5*pi-thetaR)/n_circle;
47     i = i+1;
48     n=n+1;
49 end
50 i = 0;
51 while i <= n_circle
52     x_1 = initial_radius * cos(t);
53     y_1 = initial_radius * sin(t);
54     s_prime(1,n) = x_1 + corner_ur.center(1);
55     s_prime(2,n) = y_1 + corner_ur.center(2);

```

```

56     t = t-((.5*pi+thetaR)/n.circle);
57     i = i+1;
58     n=n+1;
59 end
60 i = 0;
61 while i ≤ n.circle
62     x_1 = initial_radius * cos(t);
63     y_1 = initial_radius * sin(t);
64     s_prime(1,n) = x_1 + corner_lr.center(1);
65     s_prime(2,n) = y_1 + corner_lr.center(2);
66     t = t-((.5*pi-thetaR)/n.circle);
67     i = i+1;
68     n=n+1;
69 end
70 s_prime(:,n) = start;
71 b=1;
72 cs = transpose(s_prime);
73 plot(cs(:,1),cs(:,2))
74 %% C.S.
75 size = size(cs);
76 a=1;
77 while a≤size(1)
78     config_1(a,1) = circle_1.center(1) + cs(a,1);
79     config_1(a,2) = circle_1.center(2) + cs(a,2);
80     a = a+1;
81 end
82 a=1;
83 while a≤size(1)
84     config_2(a,1) = circle_2.center(1) + cs(a,1);
85     config_2(a,2) = circle_2.center(2) + cs(a,2);
86     a = a+1;
87 end
88 a=1;
89 while a≤size(1)
90     config_3(a,1) = circle_3.center(1) + cs(a,1);
91     config_3(a,2) = circle_3.center(2) + cs(a,2);
92     a = a+1;
93 end
94 a=1;
95 while a≤size(1)
96     config_4(a,1) = circle_4.center(1) + cs(a,1);
97     config_4(a,2) = circle_4.center(2) + cs(a,2);
98     a = a+1;
99 end
100 plot(config_1(:,1),config_1(:,2),config_2(:,1),config_2(:,2),...
101     config_3(:,1),config_3(:,2),config_4(:,1),config_4(:,2))
102 xlabel('x')
103 ylabel('y')
104 %axis([-1 50 -1 50])

```

## A.2 Configuration Space Analysis of $P_2P_2$ With 2-D Contacts

```

1 clear all
2 clc
3 clf
4
5 %% Input
6
7 ch1 = 1; %units
8 ch2 = 1; %units
9 angle = 76; %degrees
10 initial_rot = -3; %degrees
11 final_rot = 3; %degrees
12 contact_radius = .1; %units
13 initial_q = [0,0,0];
14 q_start = [-.1,0,initial_rot];
15 n_circle = 1000;
16 n_matrix_width = 300;
17 n_matrix_height = 300;
18 n_matrix_angle = 200;
19 matrix_height = .2;
20 matrix_width = .3;
21 tic
22
23 %% Initialization
24
25 rot = initial_rot;
26 q = initial_q;
27
28 %% Link 1 Creation
29 p_bl = [q(1)-.5*ch2-.5*ch1*tand(90-angle),q(2)-.5*ch1];
30 p_ul = [q(1)-.5*ch2+.5*ch1*tand(90-angle),q(2)+.5*ch1];
31 p_ur = [q(1)+.5*ch2+.5*ch1*tand(90-angle),q(2)+.5*ch1];
32 p_br = [q(1)+.5*ch2-.5*ch1*tand(90-angle),q(2)-.5*ch1];
33 P1 = [p_bl;p_ul;p_ur;p_br];
34 initialP1 = P1;
35 %% Link 2 Creation
36 anglerad = degtorad(angle);
37
38 slope3 = (p_ul(2)-p_bl(2))/(p_ul(1)-p_bl(1)); %slope of link
39
40 %creating limiting line
41 coefficients3limit = polyfit([p_ul(1), p_bl(1)], [p_ul(2), ...
    p_bl(2)], 1);
42 alimit = coefficients3limit (1);
43 blimit = coefficients3limit (2);
44
45 %creating actual link line
46 coefficients3link = ...
    polyfit([p_ul(1)-contact_radius*cosd(90-angle), ...
    p_bl(1)-contact_radius*cosd(90-angle)], ...
    [p_ul(2)+contact_radius*sind(90-angle), ...
    p_bl(2)+contact_radius*sind(90-angle)], 1);
47 alink = coefficients3link (1);
48 blink = coefficients3link (2);
49
50 xc_start = (.5*ch1 + contact_radius - blink) / alink;
51 circle_center = [xc_start,alink*xc_start+blink];
52 xc_end = (circle_center(1) + contact_radius*sind(angle));

```

```

53
54
55 % Accounting for lack of y-intercept of 90 degrees
56 if slope3 == inf
57     x3 = linspace(-.5*ch2,-.5*ch2,2);
58     y3 = [-2,2];
59 else
60     x3 = linspace(xc_end,2,2);
61     y3 = alimit*x3+blimit;
62 end
63
64 t = .5*pi;
65 i = 1;
66 circle = zeros(2,n_circle);
67 circle_center = [xc_start,alink*xc_start+blink];
68 while i ≤ n_circle
69     circle(1,i) = contact_radius * cos(t) + circle_center(1);
70     circle(2,i) = -contact_radius * sin(t) + circle_center(2);
71     t = t-(anglerad/n_circle);
72     i = i+1;
73 end
74 i = 0;
75
76 slope4 = (p_ur(2)-p_br(2))/(p_ur(1)-p_br(1));
77 coefficients4 = polyfit([p_ur(1), p_br(1)], [p_ur(2), p_br(2)], 1);
78 c = coefficients4 (1);
79 d = coefficients4 (2);
80 if slope4 == inf
81     x4 = linspace(.5*ch2,.5*ch2,2);
82     y4 = [-1000,1000];
83 else
84     x4 = linspace(.5*ch2 - .5*ch1/tand(angle),2,2);
85     y4 = c*x4+d;
86 end
87
88 x1 = linspace(-2,xc_start,2);
89 y1 = linspace(.5*ch1,.5*ch1,2);
90
91 x2 = linspace(-2,.5*ch2 - .5*ch1/tand(angle),2);
92 y2 = linspace(-.5*ch1,-.5*ch1,2);
93
94 circle_rev = fliplr(circle);
95 link2 = [x2 x4 x3(2) x3(1) circle_rev(1,:) x1(2) x1(1);y2 y4 ...
          y3(2) y3(1) circle_rev(2,:) y1(2) y1(1)];
96
97 %% Test Points
98 q = q_start;
99 xd = 1;yd = 1;
100 td = 1;
101 invalid.n_3 = 1;
102 invalid.config_3 = [];
103 valid.n_3 = 1;
104 valid.config_3 = [];
105 distance = 0;
106 distance_test = [];
107 n.distance_test_3 = 0;
108 test=0;

```



```

109 n_valid=1;
110 n_invalid=1;
111 br_x_limit = (-.5*chl-d)/slope4;
112
113 valid_config = ...
        zeros(n_matrix.width*n_matrix.height*n_matrix.angle,3);
114 invalid_config = ...
        zeros(n_matrix.width*n_matrix.height*n_matrix.angle,3);
115 for td = 1:n_matrix.angle
116     for xd = 1:n_matrix.height
117         for yd = 1:n_matrix.width
118
119             %Rotating link to current rotation
120             R = [cosd(q(3)) -sind(q(3));sind(q(3)) cosd(q(3))];
121             P1 = initialP1;
122             P1=R*P1.';
123             P1 = P1.';
124             P1(:,1) = P1(:,1)+[q(1)];
125             P1(:,2) = P1(:,2)+[q(2)];
126
127
128             %Creating the limits for points based on x and ...
                testing them
129             i=1;
130             for i = 1:4
131                 x = P1(i,1);
132                 y = P1(i,2);
133
134                 if x < xc.start
135                     y_limit_upper(i) = .5*chl;
136                     y_limit_lower(i) = -.5*chl;
137                 elseif (x ≥ xc.start) && (x < xc.end)
138                     y_limit_upper(i) = circle_center(2) - ...
                        sqrt(-circle_center(1)^2 + ...
                            contact.radius^2 + 2*circle_center(1)*x ...
                            - x^2);
139                     y_limit_lower(i) = -.5*chl;
140                 elseif (x ≥ xc.end) && (x < br_x_limit)
141                     y_limit_upper(i) = slope3 * x + blimit;
142                     y_limit_lower(i) = -.5*chl;
143                 else
144                     y_limit_upper(i) = slope3 * x + blimit;
145                     y_limit_lower(i) = c * x + d;
146                 end
147
148                 if (y ≤ y_limit_upper(i)) && (y ≥ y_limit_lower(i))
149                     isvalid(i) = 1;
150                 else
151                     isvalid(i) = 0;
152                 end
153             %             i = i+1;
154         end
155
156         %Determining if configuration is valid and archiving
157         test_valid = nnz(isvalid);
158         if test_valid == 4
159             valid_config(n_valid,:) = q;

```

```

160         n_valid = n_valid + 1;
161     else
162         invalid_config(n_invalid,:) = q;
163         n_invalid = n_invalid + 1;
164     end
165     q(1) = q(1) + matrix_width/n_matrix_width;
166     q(1) = round(q(1),12);
167
168     end
169
170     q(2) = q(2) + matrix_height/n_matrix_height;
171     q(2) = round(q(2),12);
172     q(1) = q_start(1);
173     q(1) = round(q(1),12);
174     end
175     q(1) = q_start(1);
176     q(1) = round(q(1),12);
177     q(2) = q_start(2);
178     q(2) = round(q(2),12);
179     q(3) = q(3) + (final_rot-initial_rot)/n_matrix_angle;
180     q(3) = round(q(3),12);
181
182 end
183 %% Eliminating redundant values and comparing configurations to ...
184     ideal
185     valid_config = unique(valid_config, 'rows');
186     A = arrayfun(@(x) valid_config(valid_config(:,1) == x, :), ...
187         unique(valid_config(:,1)), 'uniformoutput', false);
188     j = 1;
189     sizeA = size(A);
190     while j <= sizeA(1)
191         B = A{j};
192         xcond(j) = B(1,1);
193         t_ideal(j) = 0;
194         if xcond(j) <= 0
195             y_ideal(j) = 0;
196         else
197             y_ideal(j) = slope3*xcond(j);
198         end
199         y_max(j) = max(abs(B(:,2)));
200         t_max(j) = max(abs(B(:,3)));
201         y_error(j) = y_ideal(j)-y_max(j);
202         t_error(j) = t_ideal(j)-t_max(j);
203
204         j = j+1;
205     end
206     t_error_max = max(abs(t_error))
207
208
209     %Plotting Data
210     hold on
211     plot3(valid_config(:,1),valid_config(:,2),valid_config(:,3),'+');
212     plot(xcond,y_error)
213     plot(xcond,t_error)
214     %axis([-2 2 -2 2])

```